Study of B_c^+ decays to charmonia and three light hadrons

The LHCb collaboration

E-mail: Ivan.Belyaev@itep.ru

ABSTRACT: Using proton-proton collision data, corresponding to an integrated luminosity of $9\,\mathrm{fb}^{-1}$ collected with the LHCb detector, seven decay modes of the B_c^+ meson into a J/ψ or $\psi(2S)$ meson and three charged hadrons, kaons or pions, are studied. The decays $B_c^+ \to (\psi(2S) \to J/\psi\,\pi^+\pi^-)\pi^+$, $B_c^+ \to \psi(2S)\pi^+\pi^-\pi^+$, $B_c^+ \to J/\psi\,K^+\pi^-\pi^+$ and $B_c^+ \to J/\psi\,K^+K^-K^+$ are observed for the first time, and evidence for the $B_c^+ \to \psi(2S)K^+K^-\pi^+$, decay is found, where J/ψ and $\psi(2S)$ mesons are reconstructed in their dimuon decay modes. The ratios of branching fractions between the different B_c^+ decays are reported as well as the fractions of the decays proceeding via intermediate resonances. The results largely support the factorisation approach used for a theoretical description of the studied decays.

Contents

1 Introduction

The B_c^+ mesons are unique because they contain two different heavy-flavour quarks, charm and beauty. The ground state has a rich set of weak-decay modes since either of the heavy quarks can decay with the other behaving as a spectator quark, or both quarks can annihilate via a virtual W^+ boson. Studies of B_c^+ decay channels and measurements of their branching fractions improve the understanding of models describing strong interactions and test various effective models. Experiments at the Large Hadron Collider (LHC) have opened a new era for B_c^+ meson investigations. The high b-quark production cross-section at the LHC enables the LHCb experiment to study the production, decays and other properties of the B_c^+ meson [1–21].

Although the B_c^+ meson was discovered in 1998 by the CDF collaboration [22, 23], only two $B_c^+ \to \psi 3h^\pm$ decay channels,[1] where the symbol ψ denotes a J/ψ or a $\psi(2S)$ meson and $h^\pm$ stands for a charged kaon or pion, were previously observed by the LHCb collaboration [1, 6]. The decays of B_c^+ mesons into charmonium and light hadrons are expected to be well described by the factorisation approach [24, 25]. In this scheme, the $B_c^+ \to \psi 3h^\pm$ decay is characterised by the form factors of the $B_c^+ \to \psi W^+$ transition and the universal spectral function for the virtual W^+ boson fragmenting into light hadrons [26]. The ratios

---

[1]Inclusion of charge-conjugate states is implied throughout the paper.

of branching fractions of various $B_c^+ \to \psi 3h^\pm$ decays, based on this theoretical approach are predicted in refs. [27, 28]. A measurement of the branching fractions of the exclusive B_c^+ meson decays into the final states consisting of charmonium and light hadrons allows for precise tests of the factorisation approach.

In this paper a study of the B_c^+ meson decaying into seven final states, namely the Cabibbo-favoured $B_c^+ \to J/\psi \pi^+\pi^-\pi^+$, $B_c^+ \to \psi(2S)\pi^+\pi^-\pi^+$, $B_c^+ \to J/\psi K^+K^-\pi^+$, $B_c^+ \to \psi(2S)K^+K^-\pi^+$, $B_c^+ \to (\psi(2S) \to J/\psi \pi^+\pi^-)\pi^+$ decays, and the Cabibbo-suppressed $B_c^+ \to J/\psi K^+\pi^-\pi^+$ and $B_c^+ \to J/\psi K^+K^-K^+$ decays, is reported. The analysis is based on proton-proton (pp) collision data, corresponding to an integrated luminosity of 9 fb^{-1} collected with the LHCb detector between 2011 and 2018 at centre-of-mass energies of 7, 8, and 13 TeV. The J/ψ and $\psi(2S)$ mesons are reconstructed from their decay into two muons and the $\psi(2S) \to J/\psi \pi^+\pi^-$ channel is used for the $B_c^+ \to \psi(2S)\pi^+$ decay. The ratios of branching fractions for the decay channels under study are presented.

2   Detector and simulation

The LHCb detector [29, 30] is a single-arm forward spectrometer covering the pseudorapidity range $2 < \eta < 5$, designed for the study of particles containing b or c quarks. The detector includes a high-precision tracking system consisting of a silicon-strip vertex detector surrounding the pp interaction region [31], a large-area silicon-strip detector located upstream of a dipole magnet with a bending power of about 4 Tm, and three stations of silicon-strip detectors and straw drift tubes [32, 33] placed downstream of the magnet. The tracking system provides a measurement of the momentum of charged particles with a relative uncertainty that varies from 0.5% at low momentum to 1.0% at 200 GeV/c. The momentum scale is calibrated using samples of $J/\psi \to \mu^+\mu^-$ and $B^+ \to J/\psi K^+$ decays collected concurrently with the data sample used for this analysis [34, 35]. The relative accuracy of this procedure is estimated to be 3×10^{-4} using samples of other fully reconstructed b hadrons, Υ and K_S^0 mesons. The minimum distance between a track and a primary pp-collision vertex (PV), the impact parameter, is measured with a resolution of $(15 + 29/p_T)$ μm, where p_T is the component of the momentum transverse to the beam, in GeV/c. Different types of charged hadrons are distinguished using information from two ring-imaging Cherenkov detectors (RICH) [36]. Photons, electrons and hadrons are identified by a calorimeter system consisting of scintillating-pad and preshower detectors, an electromagnetic and a hadronic calorimeter. Muons are identified by a system composed of alternating layers of iron and multiwire proportional chambers [37].

The online event selection is performed by a trigger [38], which consists of a hardware stage, based on information from the calorimeter and muon systems, followed by a software stage, which performs a full event reconstruction. The hardware trigger selects muon candidates with high transverse momentum or dimuon candidates with a high value of the product of the individual muon p_T. In the software trigger, two oppositely-charged muons are required to form a good-quality vertex that is significantly displaced from any PV, and to have a dimuon mass exceeding 2.7 GeV/c^2.

Simulated events are used to describe the signal and to compute efficiencies needed to determine the branching fraction ratios. In the simulation, pp collisions are generated

using PYTHIA [39] with a specific LHCb configuration [40]. Decays of unstable particles are described by the EVTGEN package [41], in which final-state radiation is generated using PHOTOS [42]. The simulated decays of $B_c^+ \to J/\psi \pi^+\pi^-\pi^+$ and $B_c^+ \to \psi(2S)\pi^+\pi^-\pi^+$ are produced via an intermediate $a_1(1260)^+$ state, followed by $a_1(1260)^+ \to \rho^0\pi^+$ decay, using the phenomenological model by Berezhnoy, Likhoded, and Luchinsky [26, 28, 43] and referred to as BLL model hereafter. The simulated decays of $B_c^+ \to J/\psi K^+\pi^-\pi^+$, $B_c^+ \to J/\psi K^+K^-\pi^+$, and $B_c^+ \to \psi(2S)K^+K^-\pi^+$ include intermediate K^{*0} and $\overline{K}^{*0}$ states in the $K^+\pi^-$ and $K^-\pi^+$ systems, respectively. In the $B_c^+ \to J/\psi K^+K^-K^+$ decay several excited K^{*+} states are included, with fractions in accordance to the observations described in refs. [44, 45]. All simulated $B_c^+ \to \psi 3h^\pm$ decays are further corrected to reproduce the $\pi^+\pi^-$, $K^+\pi^-$, $K^-\pi^+$, and K^+K^- mass distributions observed in data. The interaction of the generated particles with the detector, and its response, are implemented using the GEANT4 toolkit [46, 47] as described in ref. [48]. To account for imperfections in the simulation of charged-particle reconstruction, the track-reconstruction efficiency determined from simulation is corrected using calibration samples [49].

3 Event selection

Candidate $B_c^+ \to \psi 3h^\pm$ decays are reconstructed using dimuon decays of the J/ψ and $\psi(2S)$ mesons. The criteria largely follow that described in refs. [6, 7]. The selection starts from reconstructed charged tracks of good quality that are inconsistent with being produced in a pp interaction vertex. Muon, pion and kaon candidates are identified by combining information from the RICH, calorimeter and muon detectors [50]. The muon candidates are required to have a transverse momentum larger than $550\,\mathrm{MeV}/c$. Pairs of oppositely-charged muons consistent with originating from a common vertex are combined to form $J/\psi \to \mu^+\mu^-$ and $\psi(2S) \to \mu^+\mu^-$ candidates. The reconstructed mass of the $\mu^+\mu^-$ pair is required to be in the range $3.0 < m_{\mu^+\mu^-} < 3.2$ GeV/c^2 and $3.60 < m_{\mu^+\mu^-} < 3.73$ GeV/c^2 for the J/ψ and $\psi(2S)$ candidates, respectively. The kaon candidates are required to have a transverse momentum larger than $800\,\mathrm{MeV}/c$ for the $B_c^+ \to J/\psi K^+\pi^-\pi^+$ candidates and $500\,\mathrm{MeV}/c$ for the other decay modes. The transverse momentum of pion candidates is required to be greater than $500\,\mathrm{MeV}/c$ in the $B_c^+ \to J/\psi K^+\pi^-\pi^+$ channel and $400\,\mathrm{MeV}/c$ in the other decay modes. For efficient particle identification, kaons and pions are required to have a momentum between $3.2\,\mathrm{GeV}/c$ and $150\,\mathrm{GeV}/c$. To reduce combinatorial background, only tracks that are inconsistent with originating from any reconstructed PV in the event are considered.

To form the B_c^+ candidates, the selected ψ candidates are combined with three charged tracks identified as kaons or pions, requiring a good-quality reconstructed vertex. Each B_c^+ candidate is associated with the PV that yields the smallest χ^2_{IP}, where χ^2_{IP} is defined as the difference in the vertex-fit χ^2 of a given PV reconstructed with and without the particle under consideration. To improve the mass resolution for the B_c^+ candidates, a kinematic fit [51] is performed. This fit constrains the mass of the $\mu^+\mu^-$ pair to the known mass of the J/ψ or $\psi(2S)$ meson [52] and constrains the B_c^+ candidate to originate from its associated PV. A requirement on the quality of this fit is applied to further suppress

combinatorial background. Such requirement also reduces contributions from the B_c^+ decays with the intermediate weakly-decayed hadron, such as the $B_c^+ \to J/\psi\,(D_s^+ \to 3h^\pm)$, $B_c^+ \to J/\psi\,(D^0 \to h^+h^-)K^+$, or $B_c^+ \to (B_{(s)}^0 \to J/\psi\,h^+h^-)h^+$ decays [3, 5, 15].

The measured decay time of the B_c^+ candidate, calculated with respect to the associated PV, is required to be greater than $175\,\mu m/c$ for the $B_c^+ \to J/\psi\,\pi^+\pi^-\pi^+$, $B_c^+ \to \psi(2S)\pi^+\pi^-\pi^+$, and $B_c^+ \to J/\psi\,K^+\pi^-\pi^+$ candidates, and $125\,\mu m/c$ for other decay modes. This requirement suppresses random combinations of candidates, which include tracks originating from the PV. The mass of selected B_c^+ candidates is required to be between $6.15\ GeV/c^2$ and $6.45\ GeV/c^2$.

To suppress $\psi 3h^\pm$ combinations with intermediate B_s^0, B^0, D_s^+, and D^0 mesons, a veto is applied on the mass of the corresponding two- or three-body combinations, namely ψK^+K^-, $\psi K^\mp\pi^\pm$, $K^+K^-\pi^+$, and $K^-\pi^+$. All candidates having any of these masses within a range of approximately $\pm 3\sigma_m$ around the known masses of the intermediate particles [52], where σ_m stands for the mass resolution, are rejected. For the $B_c^+ \to J/\psi\,\pi^+\pi^-\pi^+$ decay the contribution from the $B_c^+ \to (\psi(2S) \to J/\psi\,\pi^+\pi^-)\,\pi^+$ decays is removed by rejecting candidates with the $J/\psi\,\pi^+\pi^-$ mass within the range $3.67 < m_{J/\psi\,\pi^+\pi^-} < 3.70\,GeV/c^2$. For the $B_c^+ \to \psi(2S)K^+K^-\pi^+$ decay the mass of the $K^-\pi^+$ system is required to be between $0.74\,GeV/c^2$ and $1.04\,GeV/c^2$, consistent with originating from a $\overline{K}^{*0}$ meson.

Mass distributions for selected $B_c^+ \to J/\psi\,\pi^+\pi^-\pi^+$, $B_c^+ \to \psi(2S)\pi^+\pi^-\pi^+$, $B_c^+ \to J/\psi\,K^+K^-\pi^+$, $B_c^+ \to \psi(2S)K^+K^-\pi^+$, $B_c^+ \to J/\psi\,K^+\pi^-\pi^+$ and $B_c^+ \to J/\psi\,K^+K^-K^+$ candidates are shown in figure 1. Figure 2 (left) shows the mass distribution for selected $B_c^+ \to (\psi(2S) \to J/\psi\,\pi^+\pi^-)\,\pi^+$ candidates, while the corresponding mass distribution for $\psi(2S) \to J/\psi\,\pi^+\pi^-$ candidates is shown in figure 2 (right).

4 Signal yields

The yields for the $B_c^+ \to \psi 3h^\pm$ decays are determined using a simultaneous extended unbinned maximum-likelihood fit to the six mass distributions of selected $B_c^+ \to J/\psi\,\pi^+\pi^-\pi^+$, $B_c^+ \to \psi(2S)\pi^+\pi^-\pi^+$, $B_c^+ \to J/\psi\,K^+\pi^-\pi^+$, $B_c^+ \to J/\psi\,K^+K^-\pi^+$, $B_c^+ \to \psi(2S)K^+K^-\pi^+$ and $B_c^+ \to J/\psi\,K^+K^-K^+$ candidates; and a two-dimensional distribution of the $J/\psi\,\pi^+\pi^-\pi^+$ mass, $m_{J/\psi\,\pi^+\pi^-\pi^+}$, versus $J/\psi\,\pi^+\pi^-$ mass, $m_{J/\psi\,\pi^+\pi^-}$, for the $B_c^+ \to (\psi(2S) \to J/\psi\,\pi^+\pi^-)\pi^+$ candidates. To improve the resolution on the $J/\psi\,\pi^+\pi^-$ mass for the $B_c^+ \to (\psi(2S) \to J/\psi\,\pi^+\pi^-)\pi^+$ candidates and to eliminate a small correlation between $m_{J/\psi\,\pi^+\pi^-\pi^+}$ and $m_{J/\psi\,\pi^+\pi^-}$, following refs. [53, 54] the $m_{J/\psi\,\pi^+\pi^-}$ variable is computed [51] by constraining the mass of the B_c^+ candidate to its known value [52]. For each B_c^+ mass distribution the one-dimensional fit function consists of two components:

1. signal $B_c^+ \to \psi 3h^\pm$ decays parameterised by a modified Gaussian function with power-law tails on both sides of the distribution [55, 56]. The tail parameters are fixed to the values obtained from simulation;

2. random $\psi 3h^\pm$ combinations, modelled by a first-order polynomial function.
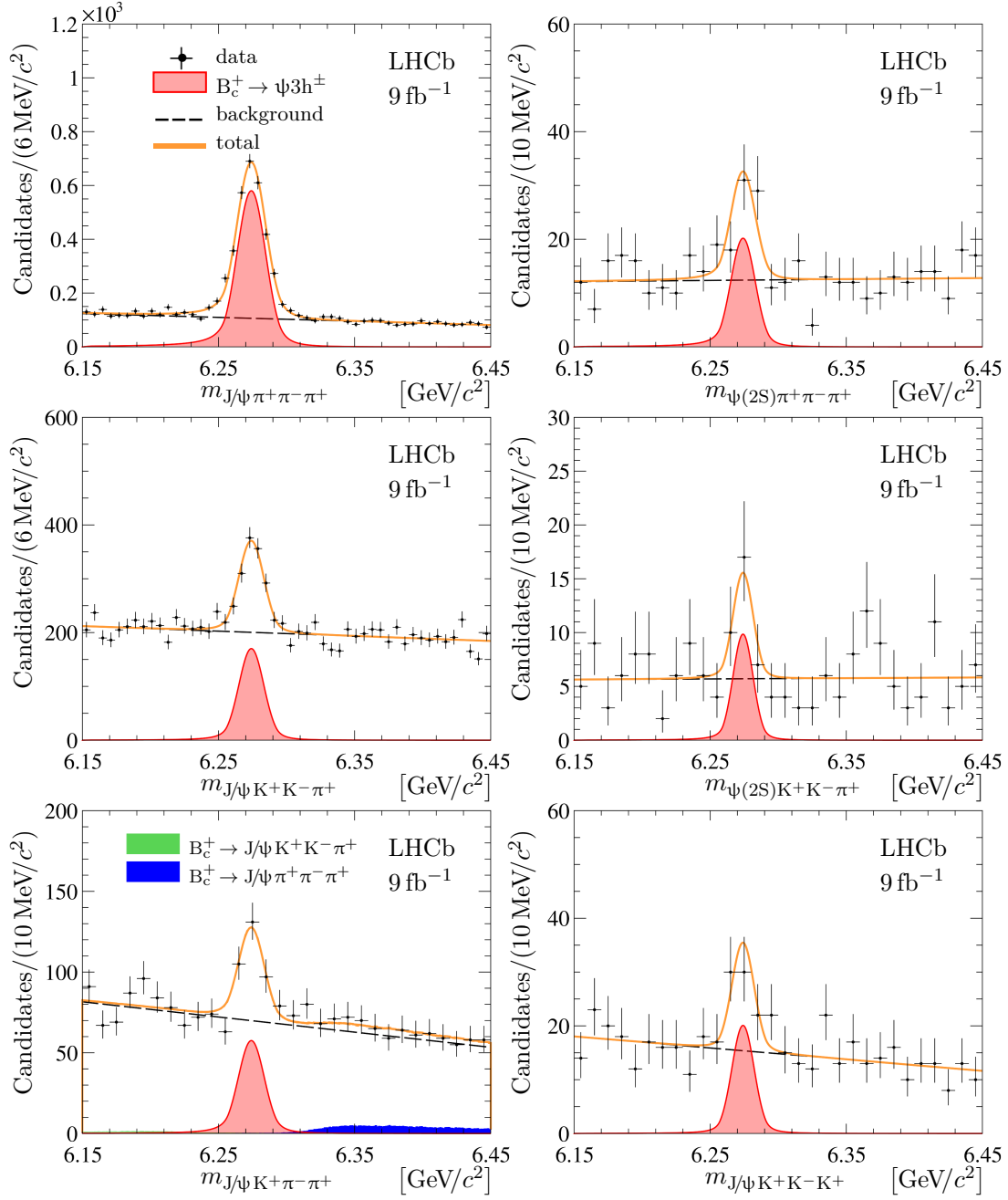
Figure 1. Mass distributions for selected $B_c^+ \to \psi 3h^\pm$ candidates. Projections of a fit, described in the text, are overlaid.

The two-dimensional fit function for the $B_c^+ \to (\psi(2S) \to J/\psi \pi^+ \pi^-)\pi^+$ channel is defined as a sum of four components:

1. signal $B_c^+ \to (\psi(2S) \to J/\psi \pi^+ \pi^-)\pi^+$ decays parameterised as a product of B_c^+ and $\psi(2S)$ signal functions modelled by a modified Gaussian function with power-law tails on both sides of the distribution [55, 56]. The tail parameters are fixed to the values obtained from simulation;
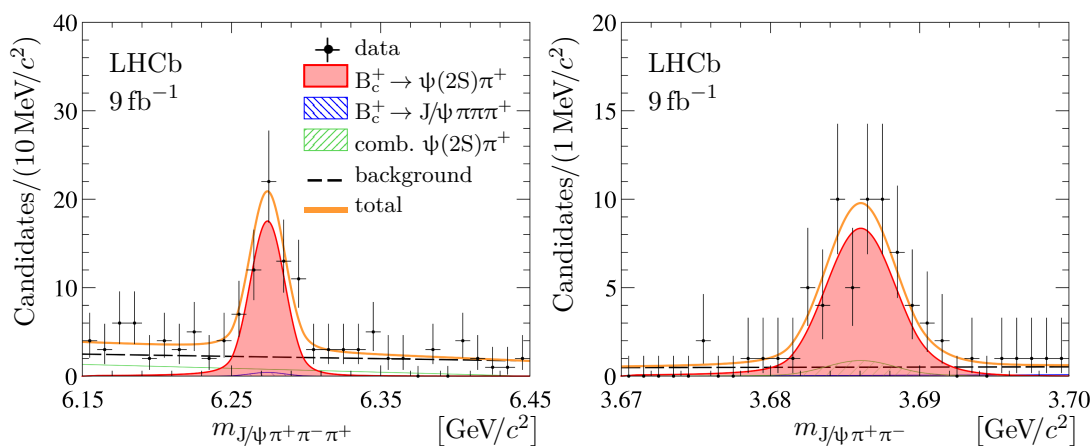
Figure 2. Distributions of the (left) $J/\psi \pi^+\pi^-\pi^+$ and (right) $J/\psi \pi^+\pi^-$ masses for selected $B_c^+ \to (\psi(2S) \to J/\psi \pi^+\pi^-)\,\pi^+$ candidates. Projections of a fit, described in the text, are overlaid. The right plot corresponds to the mass range $6.24 < m_{J/\psi \pi^+\pi^-\pi^+} < 6.31\,\mathrm{GeV}/c^2$.

2. contributions from the decays $B_c^+ \to (J/\psi \pi^+\pi^-)_{\mathrm{NR}}\,\pi^+$ without proceeding through a narrow intermediate $\psi(2S)$ state, parameterised as a product of the B_c^+ signal function and a linear function of $m_{J/\psi \pi^+\pi^-}$;

3. random combinations of $\psi(2S)$ and π^+ candidates, parameterised as a product of the $\psi(2S)$ signal template as obtained from simulation and a linear function of $m_{J/\psi \pi^+\pi^-\pi^+}$, multiplied by the two-body phase-space function [57];

4. random $J/\psi \pi^+\pi^-\pi^+$ combinations, described by a two-dimensional positive-definite first-order polynomial function.

For the Cabibbo-suppressed channel $B_c^+ \to J/\psi K^+\pi^-\pi^+$, components describing feed-down contributions from the Cabibbo-favoured $B_c^+ \to J/\psi K^+K^-\pi^+$ and $B_c^+ \to J/\psi \pi^+\pi^-\pi^+$ decays, where the kaon is misidentified as a pion or vice versa, are added into the fit function. The shapes for these contributions are taken from simulation, and their yields are constrained to the expected number of misidentified events.

For all B_c^+ signal functions, the peak-position parameter is shared between all decays and allowed to vary in the fit. The mass-resolution parameters used in the B_c^+ and $\psi(2S)$ signal functions are fixed to the values determined from simulation, and corrected by scale factors, $s_{B_c^+}$ and $s_{\psi(2S)}$, to account for a discrepancy in the mass resolution between data and simulation [53, 54, 58]. These factors are allowed to vary in the fit, and the factor $s_{B_c^+}$ is shared for all decay modes. The factor $s_{\psi(2S)}$ and the peak-position parameter for the $\psi(2S)$ signal component are constrained to the values from a previous LHCb study [53]. The mass distributions together with projections of the fit are shown in figure 1 for $B_c^+ \to J/\psi \pi^+\pi^-\pi^+$, $B_c^+ \to \psi(2S)\pi^+\pi^-\pi^+$, $B_c^+ \to J/\psi K^+K^-\pi^+$, $B_c^+ \to \psi(2S)K^+K^-\pi^+$, $B_c^+ \to J/\psi K^+\pi^-\pi^+$ and $B_c^+ \to J/\psi K^+K^-K^+$ candidates and figure 2 for the $B_c^+ \to (\psi(2S) \to J/\psi \pi^+\pi^-)\,\pi^+$ candidates. The fit parameters of interest with sta-

Decay	Yield	$\mathcal{S}\;[\sigma]$
$B_c^+ \to J/\psi\,\pi^+\pi^-\pi^+$	2750 ± 69	
$B_c^+ \to J/\psi\,K^+K^-\pi^+$	686 ± 48	
$B_c^+ \to J/\psi\,K^+K^-K^+$	43 ± 10	5.2
$B_c^+ \to J/\psi\,K^+\pi^-\pi^+$	148 ± 22	7.8
$B_c^+ \to \psi(2S)\pi^+\pi^-\pi^+$	49 ± 11	5.8
$B_c^+ \to \psi(2S)K^+K^-\pi^+$	19 ± 6	3.7
$B_c^+ \to (\psi(2S) \to J/\psi\,\pi^+\pi^-)\pi^+$	54 ± 9	11.8
Parameter	Value	
$m_{B_c^+}\quad [\,\mathrm{MeV}/c^2\,]$	6274.14 ± 0.26	
$m_{\psi(2S)}\;[\,\mathrm{MeV}/c^2\,]$	3686.05 ± 0.01	

Table 1. Parameters of interest from the simultaneous unbinned extended maximum-likelihood fit. The uncertainties are statistical only. For previously unobserved decay modes, the last column shows the statistical significance estimated using pseudoexperiments in units of standard deviations.

tistical significance of the observed signals are summarised in table 1. The resolution correction factors are found to be $s_{B_c^+} = 1.096 \pm 0.029$ and $s_{\psi(2S)} = 1.048 \pm 0.004$.

The statistical significance for previously unobserved decay modes is estimated with a large number of pseudoexperiments produced according to the background distribution observed in data. These results amount to the first observation of the decays $B_c^+ \to \psi(2S)\pi^+\pi^-\pi^+$, $B_c^+ \to J/\psi\,K^+\pi^-\pi^+$ and $B_c^+ \to J/\psi\,K^+K^-K^+$ decays, and the first evidence for the $B_c^+ \to \psi(2S)K^+K^-\pi^+$ decay. The decay $B_c^+ \to \psi(2S)\pi^+$ is confirmed using the $\psi(2S) \to J/\psi\,\pi^+\pi^-$ mode.

5 Resonance structure

The $\pi^+\pi^-\pi^+$ and $\pi^+\pi^-$ mass distributions from the $B_c^+ \to J/\psi\,\pi^+\pi^-\pi^+$ decays were previously studied in ref. [1] and were shown to be compatible with originating from a $B_c^+ \to J/\psi\,a_1(1260)^+$, followed by an $a_1(1260)^+ \to \rho^0\pi^+$ decay [26, 43]. The background-subtracted $\pi^+\pi^-\pi^+$ and $\pi^+\pi^-$ distribution for the $B_c^+ \to J/\psi\,\pi^+\pi^-\pi^+$ candidates are shown in figure 3, where the *sPlot* technique is used for background subtraction [59], using the $J/\psi\,\pi^+\pi^-\pi^+$ mass as a discriminating variable.

The $\pi^+\pi^-\pi^+$ mass distribution agrees well with the BLL model expectations [26, 28, 43]. The $\pi^+\pi^-$ mass distribution exhibits a clear peak from the ρ^0 resonance and a structure near $m_{\pi^+\pi^-} \sim 1.3\,\mathrm{GeV}/c^2$, that can be due to contributions from the decays of the wide $a_1(1260)^+$ resonance via $f_2(1270)$, $f_0(1370)$ or $\rho(1450)$ mesons [61], jointly referred to as R in the following. Unbinned non-extended maximum-likelihood fits to the $\pi^+\pi^-$ mass distribution are performed with functions that contain three terms: a component corresponding to the decay via the ρ^0 resonance; a component corresponding to the decays via S-, P-, or D-wave $\pi^+\pi^-$ resonances, and a component corresponding to B_c^+ meson decays into the $J/\psi\,\pi^+\pi^-\pi^+$ final state without resonances in the $\pi^+\pi^-$ sys-
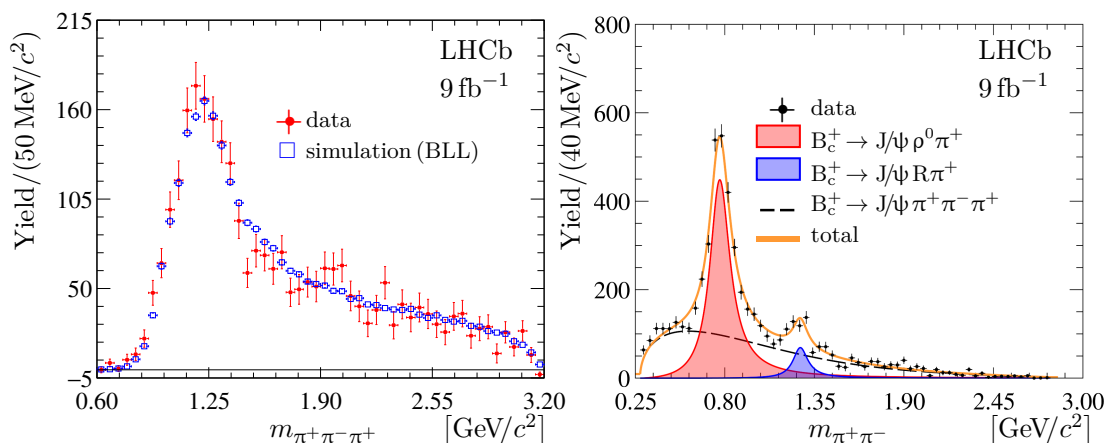
Figure 3. Background-subtracted (left) $\pi^+\pi^-\pi^+$ and (right) $\pi^+\pi^-$ mass distributions for selected $B_c^+ \to J/\psi\,\pi^+\pi^-\pi^+$ candidates. In the left plot the expectation from simulation for the $B_c^+ \to J/\psi\,a_1(1260)^+$ decays with BLL model [26, 28, 43] is overlaid.

Parameter		Value
$f_{\rho^0}^{B_c^+ \to J/\psi\,\pi^+\pi^-\pi^+}$	[%]	88.1 ± 3.0
$f_{R}^{B_c^+ \to J/\psi\,\pi^+\pi^-\pi^+}$	[%]	10.4 ± 1.4
m_R	$[\mathrm{MeV}/c^2]$	1265 ± 10
Γ_R	[MeV]	110 ± 21
$\mathcal{S}_R$	$[\sigma]$	8

Table 2. Results for parameters from the non-extended fit to the background-subtracted $\pi^+\pi^-$ mass spectrum from the $B_c^+ \to J/\psi\,\pi^+\pi^-\pi^+$ decays. The last row shows the statistical significance for the R structure estimated using Wilks' theorem [60].

tem. The resonance components are parameterised with relativistic P- and S-wave Breit-Wigner functions with Blatt-Weisskopf form factors with a meson radius of $3.5\,\mathrm{GeV}^{-1}$ [62].[2] The non-resonant component is parameterised with a product of the phase-space function describing a two-body system out of the four-body final state [57] and a positive second-order polynomial function, that accounts for the decay dynamics via the intermediate $a_1(1260)^+$ state. The ρ^0 peak position and the width are constrained to their known values [52] using Gaussian constraints, while parameters for the R structure are free to vary in the fit.

The fractions $f_{\rho^0}^{B_c^+ \to J/\psi\,\pi^+\pi^-\pi^+}$ and $f_{R}^{B_c^+ \to J/\psi\,\pi^+\pi^-\pi^+}$ of the B_c^+ meson decays into the $J/\psi\,\pi^+\pi^-\pi^+$ final state via the intermediate ρ^0 and R resonances, as well as the Breit-Wigner mass and width for the R structure, m_R and Γ_R, are shown in table 2. The results for fractions, mass and width of the resonance are stable with respect to the choice of the orbital momentum used for the Breit-Wigner function: f_{ρ^0} and f_R change by 0.002, m_R and Γ_R change by respectively $2\,\mathrm{MeV}/c^2$ and $3\,\mathrm{MeV}$, when the orbital momentum varies from

---

[2]Blatt-Weisskopf form factors with meson radius of $3.5\,\mathrm{GeV}^{-1}$ are used for all subsequent fits with relativistic Breit-Wigner functions, unless stated otherwise.
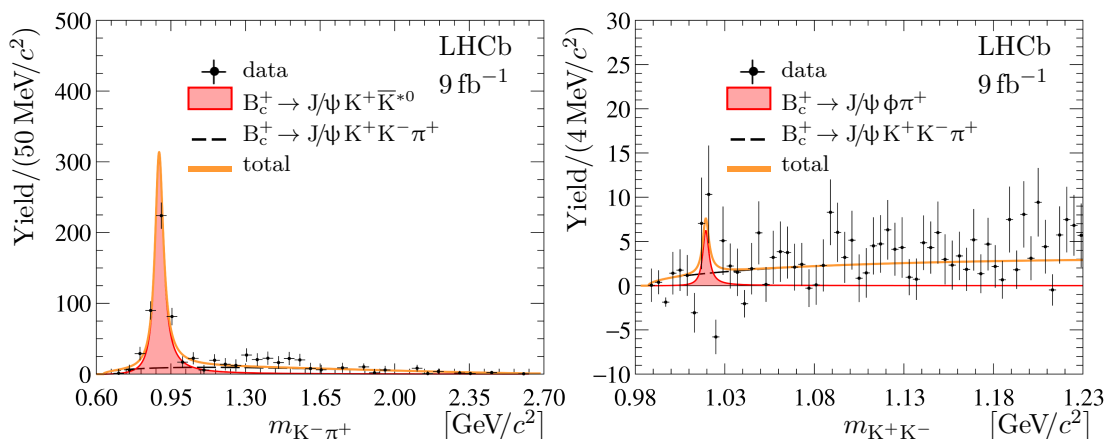
Figure 4. Background-subtracted (left) $K^-\pi^+$ and (right) K^+K^- mass distributions for selected $B_c^+ \to J/\psi K^+K^-\pi^+$ candidates. The K^+K^- mass spectrum is fitted in the full accessible K^+K^- mass region, $m_{K^+K^-} < 2.923\,\text{GeV}/c^2$. For better visibility, only a low-mass part of the spectrum is shown.

S-wave to D-wave. The statistical significance for the structure is estimated using Wilks' theorem [60] and is found to be 8 standard deviations. The obtained Breit-Wigner mass and width of the structure are consistent with those for the $f_0(1370)$ state [52]. The yield relative to the yield of decays via the ρ^0 resonance, $(11.8 \pm 1.6)\,\%$, agrees with that obtained by the CLEO collaboration from a Dalitz analysis of the $a_1(1260)^+ \to \pi^+\pi^0\pi^0$ decay [61], and is much larger than those for the $f_2(1270)$ and $\rho(1450)$ states. It allows interpretation of the R structure as the $f_0(1370)$ resonance, however alternative interpretations such as the $f_2(1270)$ or $\rho(1450)$ state are also possible.

In ref. [6] it has been demonstrated that a large fraction of the decays of the B_c^+ mesons into the $J/\psi K^+K^-\pi^+$ final state proceeds via an intermediate $\overline{K}^{*0}$ meson, while no evidence for Okubo-Zweig-Iizuka-suppressed (OZI) decays [63–65] via intermediate ϕ mesons is found. Figure 4 shows the background-subtracted $K^-\pi^+$ and K^+K^- mass distributions for the selected $B_c^+ \to J/\psi K^+K^-\pi^+$ candidates. Unbinned maximum-likelihood fits to these distributions are performed with functions consisting of two terms: a component corresponding to decays via intermediate $\overline{K}^{*0} \to K^-\pi^+$ or $\phi \to K^+K^-$ decays and a component without resonances in $K^-\pi^+$ or K^+K^- systems. The former is parameterised with a relativistic P-wave Breit-Wigner function, while the latter is parameterised with a phase-space function describing a two-body system in a four-body final state [57]. Masses and widths of the $\overline{K}^{*0}$ and ϕ resonances are allowed to vary in the fit and are Gaussian constrained to their known values [52]. Results of the fits are overlaid in figure 4. The fractions of the B_c^+ meson decays into the $J/\psi K^+K^-\pi^+$ final state via intermediate $\overline{K}^{*0}$ and ϕ resonances are found to be

$$f_{\overline{K}^{*0}}^{B_c^+ \to J/\psi K^+K^-\pi^+} = (64.5 \pm 4.7)\,\%\,,$$
$$f_{\phi}^{B_c^+ \to J/\psi K^+K^-\pi^+} = (1.6\,^{+0.7}_{-0.6})\,\%\,,$$

respectively, confirming the previous observations [6]. The upper limit at 90 (95)% confi-
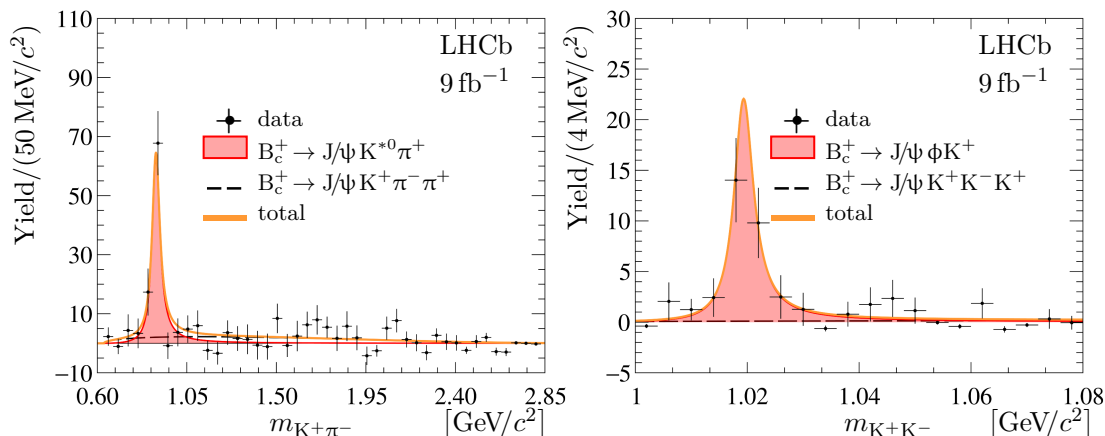
Figure 5. Background-subtracted mass distributions of (left) $K^+\pi^-$ pairs for the selected $B_c^+ \to J/\psi K^+\pi^-\pi^+$ candidates and (right) K^+K^- combinations for the selected $B_c^+ \to J/\psi K^+K^-K^+$ candidates. The K^+K^- mass spectrum is fitted in the full accessible K^+K^- mass region, $m_{K^+K^-} < 2.2\,\text{GeV}/c^2$. For better visibility, only a low-mass part of the spectrum is shown.

dence level (CL) on the fraction $f_\phi^{B_c^+ \to J/\psi K^+K^-\pi^+}$ is set as

$$f_\phi^{B_c^+ \to J/\psi K^+K^-\pi^+} < 3.9\,(4.5)\% .$$

The background-subtracted $K^+\pi^-$ and K^+K^- mass distributions for selected Cabibbo-suppressed $B_c^+ \to J/\psi K^+\pi^-\pi^+$ and $B_c^+ \to J/\psi K^+K^-K^+$ candidates are shown in figure 5. Fits to these distributions with two-component functions similar to those described above are performed and results of the fits are overlaid in figure 5. For B_c^+ decays into the $J/\psi K^+\pi^-\pi^+$ final state a large fraction proceeds via a K^{*0} meson,

$$f_{K^{*0}}^{B_c^+ \to J/\psi K^+\pi^-\pi^+} = (61.3 \pm 5.0)\%$$

and for B_c^+ decays into the $J/\psi K^+K^-K^+$ final state a dominant fraction proceeds via a ϕ meson,

$$f_\phi^{B_c^+ \to J/\psi K^+K^-K^+} = (90 \pm 19)\% .$$

All uncertainties for these resonance fractions are statistical only.

6 Ratios of branching fractions

Six ratios of branching fractions are reported in this paper,

$$\mathcal{R}_{J/\psi K^+K^-\pi^+}^{J/\psi K^+K^-K^+} \equiv \frac{\mathcal{B}(B_c^+ \to J/\psi K^+K^-K^+)}{\mathcal{B}(B_c^+ \to J/\psi K^+K^-\pi^+)} , \tag{6.1a}$$

$$\mathcal{R}_{J/\psi K^+K^-\pi^+}^{J/\psi K^+\pi^-\pi^+} \equiv \frac{\mathcal{B}(B_c^+ \to J/\psi K^+\pi^-\pi^+)}{\mathcal{B}(B_c^+ \to J/\psi K^+K^-\pi^+)} , \tag{6.1b}$$

$$\mathcal{R}_{J/\psi K^+K^-\pi^+}^{\psi(2S)K^+K^-\pi^+} \equiv \frac{\mathcal{B}(B_c^+ \to \psi(2S)K^+K^-\pi^+) \times \mathcal{B}(\psi(2S) \to \mu^+\mu^-)}{\mathcal{B}(B_c^+ \to J/\psi K^+K^-\pi^+) \times \mathcal{B}(J/\psi \to \mu^+\mu^-)} , \tag{6.1c}$$

$$\mathcal{R}_{\mathrm{J/\psi\,\pi^+\pi^-\pi^+}}^{\psi(2S)\pi^+\pi^-\pi^+} \equiv \frac{\mathcal{B}(\mathrm{B_c^+ \to \psi(2S)\pi^+\pi^-\pi^+}) \times \mathcal{B}(\psi(2S) \to \mu^+\mu^-)}{\mathcal{B}(\mathrm{B_c^+ \to J/\psi\,\pi^+\pi^-\pi^+}) \times \mathcal{B}(\mathrm{J/\psi \to \mu^+\mu^-})}\,, \tag{6.1d}$$

$$\mathcal{R}_{\mathrm{J/\psi\,\pi^+\pi^-\pi^+}}^{\psi(2S)\pi^+} \equiv \frac{\mathcal{B}(\mathrm{B_c^+ \to \psi(2S)\pi^+}) \times \mathcal{B}(\psi(2S) \to \mathrm{J/\psi}\,\pi^+\pi^-)}{\mathcal{B}(\mathrm{B_c^+ \to J/\psi\,\pi^+\pi^-\pi^+})}\,, \tag{6.1e}$$

$$\mathcal{R}_{\mathrm{J/\psi\,\pi^+\pi^-\pi^+}}^{\mathrm{J/\psi\,K^+K^-\pi^+}} \equiv \frac{\mathcal{B}(\mathrm{B_c^+ \to J/\psi\,K^+K^-\pi^+})}{\mathcal{B}(\mathrm{B_c^+ \to J/\psi\,\pi^+\pi^-\pi^+})}\,, \tag{6.1f}$$

where decays are paired to give the largest cancellation of systematic uncertainties. Each ratio of branching fractions for $\mathrm{B_c^+ \to X}$ and $\mathrm{B_c^+ \to Y}$ decay modes, $\mathcal{R}_\mathrm{Y}^\mathrm{X}$, is calculated as

$$\mathcal{R}_\mathrm{Y}^\mathrm{X} = \frac{N_\mathrm{X}}{N_\mathrm{Y}} \times \frac{\varepsilon_\mathrm{Y}}{\varepsilon_\mathrm{X}}\,, \tag{6.2}$$

where N is the signal yield reported in table 1 and ε denotes the efficiency of the corresponding decay. The efficiency is defined as the product of geometric acceptance, reconstruction, selection, hadron identification and trigger efficiencies. All of these contributions, except that of the hadron-identification efficiency, are determined using simulated samples, corrected as described above. The hadron-identification efficiency is calculated from single-track hadron identification efficiencies for kaons and pions, determined from large calibration samples of $\mathrm{D^{*+} \to (D^0 \to K^-\pi^+)\,\pi^+}$, $\mathrm{K_S^0 \to \pi^+\pi^-}$ and $\mathrm{D_s^+ \to (\phi \to K^+K^-)\,\pi^+}$ decays [36, 66].

The measured ratios of branching fractions are

$$\mathcal{R}_{\mathrm{J/\psi\,K^+K^-\pi^+}}^{\mathrm{J/\psi\,K^+K^-K^+}} = (7.0 \pm 1.8) \times 10^{-2}\,,$$

$$\mathcal{R}_{\mathrm{J/\psi\,K^+K^-\pi^+}}^{\mathrm{J/\psi\,K^+\pi^-\pi^+}} = 0.35 \pm 0.06\,,$$

$$\mathcal{R}_{\mathrm{J/\psi\,K^+K^-\pi^+}}^{\psi(2S)\mathrm{K^+K^-\pi^+}} = (3.7 \pm 1.2) \times 10^{-2}\,,$$

$$\mathcal{R}_{\mathrm{J/\psi\,\pi^+\pi^-\pi^+}}^{\psi(2S)\pi^+\pi^-\pi^+} = (1.9 \pm 0.4) \times 10^{-2}\,,$$

$$\mathcal{R}_{\mathrm{J/\psi\,\pi^+\pi^-\pi^+}}^{\psi(2S)\pi^+} = (3.5 \pm 0.6) \times 10^{-2}\,,$$

$$\mathcal{R}_{\mathrm{J/\psi\,\pi^+\pi^-\pi^+}}^{\mathrm{J/\psi\,K^+K^-\pi^+}} = 0.185 \pm 0.013\,,$$

where uncertainties are statistical only and correlation coefficients are listed in table 7. Systematic uncertainties are discussed in section 7.

7 Systematic uncertainties

The decay channels under study have similar kinematics and topologies, therefore a large part of systematic uncertainties cancels in the branching fraction ratios $\mathcal{R}_\mathrm{Y}^\mathrm{X}$. The remaining contributions to the systematic uncertainty are summarised in table 3 and discussed below.

An important source of systematic uncertainty on the ratios arises from the imperfect knowledge of the shapes of signal and background components used in the fits. To estimate this uncertainty, several alternative models are tested. For the $\mathrm{B_c^+}$ and $\psi(2S)$ signal shapes an Apollonios function [67] is employed as an alternative model. The degree of the polynomials used in the fits is increased by one. The systematic uncertainty related

Source	Uncertainty [%]
Fit model	
Signal shape	$< 0.1 - 2.8$
Background shape	$0.2 - 3.7$
B_c^+ decay model	$< 0.1 - 0.3$
Efficiency corrections	$< 0.1 - 1.6$
Trigger efficiency	1.1
Data-simulation difference	3.0
Size of simulated sample	$0.6 - 2.1$
Total	$3.3 - 5.6$

Table 3. Ranges of relative systematic uncertainties for the ratios of branching fractions $\mathcal{R}_Y^X$. The total systematic uncertainty is the quadratic sum of individual contributions.

to the fit model is estimated by pseudoexperiments with the baseline fit model and fitted with alternative models. Each pseudoexperiment is approximately 100 times larger than the data sample. The maximal deviations in the ratios of the signal yields with respect to the baseline model do not exceed 2.8% for variation of the signal model and 3.7% for variation of background model, and are taken as systematic uncertainties in the ratios $\mathcal{R}_Y^X$.

The simulated $B_c^+ \to \psi 3h^\pm$ decays are corrected to reproduce the two-dimensional $\pi^+\pi^-$, $K^+\pi^-$, $K^-\pi^+$, and K^+K^- mass distributions observed in data. The effect of statistical uncertainties for the reference distributions in data on the determination of the efficiencies is studied using pseudoexperiments. Variations of the efficiency ratios, and subsequent changes in the ratios $\mathcal{R}_Y^X$, are found to be not exceeding 0.3%. These changes are taken as systematic uncertainties related to the B_c^+ decay model.

An additional uncertainty arises from differences between data and simulation, in particular differences in the reconstruction efficiency of charged-particle tracks. The track-finding efficiencies obtained from simulation are corrected using data calibration samples [49]. The uncertainties related to the correction factors, together with the uncertainty in the hadron-identification efficiency due to the finite size of the calibration samples [36, 66], are propagated to the ratio of total efficiencies using pseudoexperiments. The obtained systematic uncertainty for the $\mathcal{R}_Y^X$ ratios do not exceed 1.6%.

The systematic uncertainty related to the trigger efficiency is estimated by comparing the ratios of trigger efficiencies in data and simulation using large samples of the $B^+ \to J/\psi K^+$ and $B^+ \to \psi(2S)K^+$ decays [68]. Another source of uncertainty is a potential disagreement between data and simulation in the estimation of efficiencies, due to possible effects not considered above. This is studied by varying the selection criteria in ranges that lead up to a $\pm 20\%$ change in the measured signal yields. For this study, the high yield $B_c^+ \to J/\psi \pi^+\pi^-\pi^+$ data sample is used. The resulting difference between the efficiencies estimated using data and simulation does not exceed 3.0%, which is taken as a systematic uncertainty for the ratios $\mathcal{R}_Y^X$. The last systematic uncertainty considered for the ratios $\mathcal{R}_Y^X$ is due to the finite size of the simulated samples and it varies between 0.6% and 2.1%.

Fraction	Uncertainty [%]
$f_{\rho^0}^{B_c^+ \to J/\psi\,\pi^+\pi^-\pi^+}$	$+12.0$ -0.3
$f_R^{B_c^+ \to J/\psi\,\pi^+\pi^-\pi^+}$	$+8.0$ -1.2
$f_{\overline{K}^{*0}}^{B_c^+ \to J/\psi\,K^+K^-\pi^+}$	$+3.9$ -4.8
$f_{K^{*0}}^{B_c^+ \to J/\psi\,K^+\pi^-\pi^+}$	$+7.7$ -0.3
$f_\phi^{B_c^+ \to J/\psi\,K^+K^-K^+}$	$+5.0$ -7.0

Table 4. Systematic uncertainties for the fractions of the decays via resonances.

Systematic uncertainties for the fractions of decays via resonances are estimated by variation of the fit models. In particular, the meson radii are varied between 1.5 and $5\,\mathrm{GeV}^{-1}$, the degree of polynomial functions is varied from one to three and, for $B_c^+ \to J/\psi\,\pi^+\pi^-\pi^+$ decays, the Gounaris-Sakurai function [69] is used for the ρ^0 meson parameterisation. For each alternative model the fit fraction is determined and the maximal difference in the fractions with respect to the default fit model is taken as a corresponding systematic uncertainty. The systematic uncertainties for the fractions are summarised in table 4. For the fraction $f_\phi^{B_c^+ \to J/\psi\,K^+K^-\pi^+}$, the upper limits are estimated for each alternative model, and the largest value is taken. The upper limit at $90\,(95)\%$ CL that accounts for the systematic uncertainty is $f_\phi^{B_c^+ \to J/\psi\,K^+K^-\pi^+} < 4.2\,(4.8)\%$.

8 Results and summary

The $B_c^+ \to \psi 3h^\pm$ decays are studied using proton-proton collision data, corresponding to an integrated luminosity of $9\,\mathrm{fb}^{-1}$, collected with the LHCb detector. The first observation of the decays $B_c^+ \to \psi(2S)\pi^+\pi^-\pi^+$, $B_c^+ \to J/\psi\,K^+\pi^-\pi^+$ and $B_c^+ \to J/\psi\,K^+K^-K^+$ is reported. The decay $B_c^+ \to \psi(2S)\pi^+$ is confirmed using $\psi(2S) \to J/\psi\,\pi^+\pi^-$ mode and the first evidence for the $B_c^+ \to \psi(2S)K^+K^-\pi^+$ decay is obtained with a significance of 3.7 standard deviations.

The three-pion mass distribution for the $B_c^+ \to J/\psi\,\pi^+\pi^-\pi^+$ decays is found to be consistent with a BLL model for the $B_c^+ \to J/\psi\,a_1(1260)^+$ decay based on the factorisation approach [26, 28, 43], in agreement with previous studies [1]. The presence of the intermediate axial $a_1(1260)^+$ meson in this decay is further supported by a large fraction of the $B_c^+ \to J/\psi\,\pi^+\pi^-\pi^+$ decays proceeding via the intermediate ρ^0 resonance

$$f_{\rho^0}^{B_c^+ \to J/\psi\,\pi^+\pi^-\pi^+} = \left(88.1 \pm 3.0^{+12.0}_{-0.3}\right)\%,$$

and the observation of a structure in the $\pi^+\pi^-$ mass spectrum, consistent with the $a_1(1260)^+ \to \left(f_0(1370) \to \pi^+\pi^-\right)\pi^+$ decay. The fraction of the $B_c^+ \to J/\psi\,\pi^+\pi^-\pi^+$ decays proceeding via this intermediate state is found to be

$$f_R^{B_c^+ \to J/\psi\,\pi^+\pi^-\pi^+} = \left(10.4 \pm 1.4^{+8.0}_{-1.2}\right)\%,$$

Ratio	Value	Prediction, measurement	Reference
$\mathcal{R}^{\psi(2S)K^+K^-\pi^+}_{\psi(2S)\pi^+\pi^-\pi^+}$	$0.37 \pm 0.15 \pm 0.01$	0.16	BLL [27, 28]
$\mathcal{R}^{J/\psi K^+\pi^-\pi^+}_{J/\psi K^+K^-\pi^+}$	$0.35 \pm 0.06 \pm 0.01$	0.37	BLL [27]
$\mathcal{R}^{J/\psi K^+\pi^-\pi^+}_{J/\psi \pi^+\pi^-\pi^+}$	$(6.4 \pm 1.0 \pm 0.2) \times 10^{-2}$	7.7×10^{-2}	BLL [27]
$\mathcal{R}^{J/\psi K^+K^-\pi^+}_{J/\psi \pi^+\pi^-\pi^+}$	$0.185 \pm 0.013 \pm 0.006$	0.21	BLL [27, 28]
$\mathcal{R}^{\psi(2S)\pi^+}_{J/\psi K^+K^-\pi^+}$	$0.19 \pm 0.03 \pm 0.01$	0.18 ± 0.04	LHCb [6, 11]
$\mathcal{R}^{\psi(2S)\pi^+}_{J/\psi \pi^+\pi^-\pi^+}$	$(3.5 \pm 0.6 \pm 0.2) \times 10^{-2}$	$(3.9 \pm 0.9) \times 10^{-2}$	LHCb [1, 11]
$\mathcal{R}^{J/\psi K^+K^-\pi^+}_{J/\psi \pi^+\pi^-\pi^+}$	$0.185 \pm 0.013 \pm 0.006$	0.22 ± 0.06	LHCb [1, 6]

Table 5. Comparison of the measured ratios $\mathcal{R}^X_Y$ with their theoretical predictions or derivations from previous measurements.

which agrees with the value of $(7.40 \pm 2.71 \pm 1.26)\,\%$, obtained by the CLEO collaboration for the fraction of the $a_1(1260)^+ \to \pi^+\pi^0\pi^0$ decays proceeding via intermediate $f_0(1370)$ state [61].

The fraction of the $B_c^+ \to J/\psi K^+K^-\pi^+$ decays proceeding via intermediate $\overline{K}^{*0}$ state is measured to be

$$f^{B_c^+ \to J/\psi K^+K^-\pi^+}_{\overline{K}^{*0}} = \left(64.5 \pm 4.7 \, ^{+\,3.9}_{-\,4.8}\right)\%,$$

while no evidence for OZI-suppressed decays $B_c^+ \to J/\psi \left(\phi \to K^+K^-\right)\pi^+$ is found and the upper limit at $90\,(95)\%$ CL of the corresponding fraction of the $B_c^+ \to J/\psi K^+K^-\pi^+$ decays proceeding via intermediate ϕ meson is set to be

$$f^{B_c^+ \to J/\psi K^+K^-\pi^+}_{\phi} < 4.2\,(4.8)\%.$$

Both results are in agreement with the previous study by the LHCb collaboration [6]. For the $B_c^+ \to J/\psi K^+\pi^-\pi^+$ and $B_c^+ \to J/\psi K^+K^-K^+$ decays large fractions of decays via intermediate K^{*0} and ϕ resonances, respectively, are found

$$f^{B_c^+ \to J/\psi K^+\pi^-\pi^+}_{K^{*0}} = \left(61.3 \pm 5.0 \, ^{+\,7.7}_{-\,0.3}\right)\%,$$

$$f^{B_c^+ \to J/\psi K^+K^-K^+}_{\phi} = \left(90 \pm 19 \, ^{+\,5}_{-\,7}\right)\%.$$

The six ratios of branching fractions are measured as

$$\mathcal{R}^{J/\psi K^+K^-K^+}_{J/\psi K^+K^-\pi^+} = (7.0 \pm 1.8 \pm 0.2) \times 10^{-2},$$

$$\mathcal{R}^{J/\psi K^+\pi^-\pi^+}_{J/\psi K^+K^-\pi^+} = 0.35 \pm 0.06 \pm 0.01,$$

$$\mathcal{R}^{\psi(2S)K^+K^-\pi^+}_{J/\psi K^+K^-\pi^+} = (3.7 \pm 1.2 \pm 0.1) \times 10^{-2},$$

$$\mathcal{R}^{\psi(2S)\pi^+\pi^-\pi^+}_{J/\psi \pi^+\pi^-\pi^+} = (1.9 \pm 0.4 \pm 0.1) \times 10^{-2}$$

$$\mathcal{R}^{\psi(2S)\pi^+}_{J/\psi \pi^+\pi^-\pi^+} = (3.5 \pm 0.6 \pm 0.2) \times 10^{-2},$$

$$\mathcal{R}^{J/\psi K^+K^-\pi^+}_{J/\psi \pi^+\pi^-\pi^+} = 0.185 \pm 0.013 \pm 0.006,$$

	Value $\left[10^{-2}\right]$	Reference
$\mathcal{R}_{\mathrm{J/\psi\,K^+K^-\pi^+}}^{\mathrm{J/\psi\,K^+K^-K^+}}$	$7.0 \pm 1.8 \pm 0.2$	This paper
$\mathcal{R}_{\mathrm{J/\psi\,\pi^+\pi^-\pi^+}}^{\mathrm{J/\psi\,K^+\pi^-\pi^+}}$	$6.4 \pm 1.0 \pm 0.2$	This paper
$\dfrac{\mathcal{B}(\mathrm{B_c^+ \to J/\psi\,K^+})}{\mathcal{B}(\mathrm{B_c^+ \to J/\psi\,\pi^+})}$	7.9 ± 0.8	[14]
$\dfrac{\mathcal{B}(\mathrm{B^+ \to \overline{D}^0 K^+\pi^-\pi^+})}{\mathcal{B}(\mathrm{B^+ \to \overline{D}^0 \pi^+\pi^-\pi^+})}$	9.3 ± 5.1	[52, 70]
$\dfrac{\mathcal{B}(\mathrm{B^0 \to D^- K^+\pi^-\pi^+})}{\mathcal{B}(\mathrm{B^0 \to D^- \pi^+\pi^-\pi^+})}$	5.8 ± 1.5	[52, 70]
$\dfrac{\mathcal{B}(\mathrm{B^0 \to D^{*-} K^+\pi^-\pi^+})}{\mathcal{B}(\mathrm{B^0 \to D^{*-} \pi^+\pi^-\pi^+})}$	6.5 ± 0.6	[52, 71]
$\dfrac{\mathcal{B}(\mathrm{B_s^0 \to D_s^- K^+\pi^-\pi^+})}{\mathcal{B}(\mathrm{B_s^0 \to D_s^- \pi^+\pi^-\pi^+})}$	5.2 ± 1.3	[52, 72]

Table 6. Comparison of the measured ratios of branching fractions for the Cabibbo-suppressed and Cabibbo-favoured decays with the ratios of branching fraction for similar decays of $\mathrm{B_c^+}$, $\mathrm{B^+}$, $\mathrm{B^0}$ and $\mathrm{B_s^0}$ mesons [14, 52, 70–72].

where the first uncertainty is statistical and the second systematic. Correlation coefficients for statistical and systematic uncertainties are given in appendix A. The ratios of branching fractions from this measurement are compared in table 5 with either theoretical predictions [27, 28] or derivations from previous LHCb measurements [1, 6, 11].

The ratio of branching fractions for the $\mathrm{B_c^+}$ decays via $\psi(2\mathrm{S})$ and $\mathrm{J/\psi}$ mesons, $\mathcal{R}_{\mathrm{J/\psi\,K^+K^-\pi^+}}^{\psi(2\mathrm{S})\mathrm{K^+K^-\pi^+}}$, agrees with the known ratio of branching fractions for the $\mathrm{B_c^+} \to \psi(2\mathrm{S})\pi^+$ and $\mathrm{B_c^+} \to \mathrm{J/\psi}\,\pi^+$ decays $\mathcal{R}_{\mathrm{J/\psi\,\pi^+}}^{\psi(2\mathrm{S})\pi^+} = (3.54 \pm 0.43) \times 10^{-2}$ [11], however the similar ratio for the $\mathrm{B_c^+} \to \psi(2\mathrm{S})\pi^+\pi^-\pi^+$ and $\mathrm{B_c^+} \to \mathrm{J/\psi}\,\pi^+\pi^-\pi^+$ channels, $\mathcal{R}_{\mathrm{J/\psi\,\pi^+\pi^-\pi^+}}^{\psi(2\mathrm{S})\pi^+\pi^-\pi^+}$, is in tension, at 2.8 standard deviations, with the measured ratio $\mathcal{R}_{\mathrm{J/\psi\,\pi^+}}^{\psi(2\mathrm{S})\pi^+}$ [11]. The ratio $\mathcal{R}_{\mathrm{J/\psi\,K^+K^-\pi^+}}^{\mathrm{J/\psi\,K^+K^-K^+}}$ of branching fractions for the Cabibbo-suppressed $\mathrm{B_c^+} \to \mathrm{J/\psi}\,\mathrm{K^+K^-K^+}$ and Cabibbo-favoured $\mathrm{B_c^+} \to \mathrm{J/\psi}\,\mathrm{K^+K^-\pi^+}$ decays agrees within uncertainties with the similar ratio $\mathcal{R}_{\mathrm{J/\psi\,\pi^+\pi^-\pi^+}}^{\mathrm{J/\psi\,K^+\pi^-\pi^+}}$ and the known ratio of branching fractions for the Cabibbo-suppressed $\mathrm{B_c^+} \to \mathrm{J/\psi}\,\mathrm{K^+}$ and Cabibbo-favoured $\mathrm{B_c^+} \to \mathrm{J/\psi}\,\pi^+$ decays [14]. The ratios $\mathcal{R}_{\mathrm{J/\psi\,K^+K^-\pi^+}}^{\mathrm{J/\psi\,K^+K^-K^+}}$ and $\mathcal{R}_{\mathrm{J/\psi\,\pi^+\pi^-\pi^+}}^{\mathrm{J/\psi\,K^+\pi^-\pi^+}}$ also agree with the ratios of branching fraction for the multibody decays of $\mathrm{B^+}$, $\mathrm{B^0}$ and $\mathrm{B_s^0}$ mesons, see table 6. This pattern supports the factorisation hypothesis for the $\mathrm{B_c^+} \to \psi 3\mathrm{h}^{\pm}$ decays.

Acknowledgments

A Correlation matrices

Correlation coefficients for the measured ratios $\mathcal{R}^X_Y$ are shown in tables 7 and 8 for statistical and systematic uncertainties, respectively.

	$\mathcal{R}^{J/\psi\,K^+\pi^-\pi^+}_{J/\psi\,K^+K^-\pi^+}$	$\mathcal{R}^{\psi(2S)K^+K^-\pi^+}_{J/\psi\,K^+K^-\pi^+}$	$\mathcal{R}^{\psi(2S)\pi^+\pi^-\pi^+}_{J/\psi\,\pi^+\pi^-\pi^+}$	$\mathcal{R}^{\psi(2S)\pi^+}_{J/\psi\,\pi^+\pi^-\pi^+}$	$\mathcal{R}^{J/\psi\,K^+K^-\pi^+}_{J/\psi\,\pi^+\pi^-\pi^+}$
$\mathcal{R}^{J/\psi\,K^+K^-K^+}_{J/\psi\,K^+K^-\pi^+}$	-13	$+0$	-8	$+2$	-24
$\mathcal{R}^{J/\psi\,K^+\pi^-\pi^+}_{J/\psi\,K^+K^-\pi^+}$		$+4$	-7	$+1$	-33
$\mathcal{R}^{\psi(2S)K^+K^-\pi^+}_{J/\psi\,K^+K^-\pi^+}$			-1	-3	-15
$\mathcal{R}^{\psi(2S)\pi^+\pi^-\pi^+}_{J/\psi\,\pi^+\pi^-\pi^+}$				-4	$+12$
$\mathcal{R}^{\psi(2S)\pi^+}_{J/\psi\,\pi^+\pi^-\pi^+}$					$+0$

Table 7. Off-diagonal correlation coefficients ([%]) for statistical uncertainties for the measured ratios $\mathcal{R}^X_Y$.

	$\mathcal{R}^{J/\psi\,K^+\pi^-\pi^+}_{J/\psi\,K^+K^-\pi^+}$	$\mathcal{R}^{\psi(2S)K^+K^-\pi^+}_{J/\psi\,K^+K^-\pi^+}$	$\mathcal{R}^{\psi(2S)\pi^+\pi^-\pi^+}_{J/\psi\,\pi^+\pi^-\pi^+}$	$\mathcal{R}^{\psi(2S)\pi^+}_{J/\psi\,\pi^+\pi^-\pi^+}$	$\mathcal{R}^{J/\psi\,K^+K^-\pi^+}_{J/\psi\,\pi^+\pi^-\pi^+}$
$\mathcal{R}^{J/\psi\,K^+K^-K^+}_{J/\psi\,K^+K^-\pi^+}$	$+39$	$+18$	$+2$	-10	-52
$\mathcal{R}^{J/\psi\,K^+\pi^-\pi^+}_{J/\psi\,K^+K^-\pi^+}$		$+27$	-7	-4	-60
$\mathcal{R}^{\psi(2S)K^+K^-\pi^+}_{J/\psi\,K^+K^-\pi^+}$			$+9$	-20	-59
$\mathcal{R}^{\psi(2S)\pi^+\pi^-\pi^+}_{J/\psi\,\pi^+\pi^-\pi^+}$				$+27$	$+30$
$\mathcal{R}^{\psi(2S)\pi^+}_{J/\psi\,\pi^+\pi^-\pi^+}$					$+37$

Table 8. Off-diagonal correlation coefficients ([%]) for systematic uncertainties for the measured ratios $\mathcal{R}^X_Y$.

References

[1] LHCb collaboration, *First observation of the decay $B_c^+ \to J/\psi\pi^+\pi^-\pi^+$*, *Phys. Rev. Lett.* **108** (2012) 251802 [`arXiv:1204.0079`] [INSPIRE].

[2] LHCb collaboration, *Observation of the decay $B_c^+ \to \psi(2S)\pi^+$*, *Phys. Rev. D* **87** (2013) 071103 [`arXiv:1303.1737`] [INSPIRE].

[3] LHCb collaboration, *Observation of $B_c^+ \to J/\psi D_s^+$ and $B_c^+ \to J/\psi D_s^{*+}$ decays*, *Phys. Rev. D* **87** (2013) 112012 [*Addendum ibid.* **89** (2014) 019901] [`arXiv:1304.4530`] [INSPIRE].

[4] LHCb collaboration, *First observation of the decay $B_c^+ \to J/\psi K^+$*, *JHEP* **09** (2013) 075 [`arXiv:1306.6723`] [INSPIRE].

[5] LHCb collaboration, *Observation of the Decay $B_c^+ \to B_s^0\pi^+$*, *Phys. Rev. Lett.* **111** (2013) 181801 [`arXiv:1308.4544`] [INSPIRE].

[6] LHCb collaboration, *Observation of the decay $B_c^+ \to J/\psi K^+K^-\pi^+$*, *JHEP* **11** (2013) 094 [`arXiv:1309.0587`] [INSPIRE].

[7] LHCb collaboration, *Evidence for the decay $B_c^+ \to J/\psi 3\pi^+2\pi^-$*, *JHEP* **05** (2014) 148 [`arXiv:1404.0287`] [INSPIRE].

[8] LHCb collaboration, *First observation of a baryonic B_c^+ decay*, *Phys. Rev. Lett.* **113** (2014) 152003 [`arXiv:1408.0971`] [INSPIRE].

[9] LHCb collaboration, *Measurement of B_c^+ production in proton-proton collisions at $\sqrt{s} = 8$ TeV*, *Phys. Rev. Lett.* **114** (2015) 132001 [`arXiv:1411.2943`] [INSPIRE].

[10] LHCb collaboration, *Measurement of the lifetime of the B_c^+ meson using the $B_c^+ \to J/\psi\pi^+$ decay mode*, *Phys. Lett. B* **742** (2015) 29 [`arXiv:1411.6899`] [INSPIRE].

[11] LHCb collaboration, *Measurement of the branching fraction ratio $\mathcal{B}(B_c^+ \to \psi(2S)\pi^+)/\mathcal{B}(B_c^+ \to J/\psi\pi^+)$*, *Phys. Rev. D* **92** (2015) 072007 [`arXiv:1507.03516`] [INSPIRE].

[12] LHCb collaboration, *Search for B_c^+ decays to the $p\bar{p}\pi^+$ final state*, *Phys. Lett. B* **759** (2016) 313 [`arXiv:1603.07037`] [INSPIRE].

[13] LHCb collaboration, *Study of B_c^+ decays to the $K^+K^-\pi^+$ final state and evidence for the decay $B_c^+ \to \chi_{c0}\pi^+$*, *Phys. Rev. D* **94** (2016) 091102 [`arXiv:1607.06134`] [INSPIRE].

[14] LHCb collaboration, *Measurement of the ratio of branching fractions $\mathcal{B}(B_c^+ \to J/\psi K^+)/\mathcal{B}(B_c^+ \to J/\psi\pi^+)$*, *JHEP* **09** (2016) 153 [`arXiv:1607.06823`] [INSPIRE].

[15] LHCb collaboration, *Observation of $B_c^+ \to J/\psi D^{(*)}K^{(*)}$ decays*, *Phys. Rev. D* **95** (2017) 032005 [`arXiv:1612.07421`] [INSPIRE].

[16] LHCb collaboration, *Observation of $B_c^+ \to D^0K^+$ decays*, *Phys. Rev. Lett.* **118** (2017) 111803 [`arXiv:1701.01856`] [INSPIRE].

[17] LHCb collaboration, *Measurement of the ratio of branching fractions $\mathcal{B}(B_c^+ \to J/\psi\tau^+\nu_\tau)/\mathcal{B}(B_c^+ \to J/\psi\mu^+\nu_\mu)$*, *Phys. Rev. Lett.* **120** (2018) 121801 [`arXiv:1711.05623`] [INSPIRE].

[18] LHCb collaboration, *Search for B_c^+ decays to two charm mesons*, *Nucl. Phys. B* **930** (2018) 563 [arXiv:1712.04702] [INSPIRE].

[19] LHCb collaboration, *Measurement of the B_c^- meson production fraction and asymmetry in 7 and 13 TeV pp collisions*, *Phys. Rev. D* **100** (2019) 112006 [arXiv:1910.13404] [INSPIRE].

[20] LHCb collaboration, *Precision measurement of the B_c^+ meson mass*, *JHEP* **07** (2020) 123 [arXiv:2004.08163] [INSPIRE].

[21] LHCb collaboration, *Updated search for B_c^+ decays to two charm mesons*, *JHEP* **12** (2021) 117 [arXiv:2109.00488] [INSPIRE].

[22] CDF collaboration, *Observation of the B_c meson in $p\bar{p}$ collisions at $\sqrt{s} = 1.8$ TeV*, *Phys. Rev. Lett.* **81** (1998) 2432 [hep-ex/9805034] [INSPIRE].

[23] CDF collaboration, *Observation of B_c mesons in $p\bar{p}$ collisions at $\sqrt{s} = 1.8$ TeV*, *Phys. Rev. D* **58** (1998) 112004 [hep-ex/9804014] [INSPIRE].

[24] M. Bauer, B. Stech and M. Wirbel, *Exclusive nonleptonic decays of D, $D_{(s)}$, and B mesons*, *Z. Phys. C* **34** (1987) 103 [INSPIRE].

[25] M. Wirbel, *Description of weak decays of D and B mesons*, *Prog. Part. Nucl. Phys.* **21** (1988) 33 [INSPIRE].

[26] A.K. Likhoded and A.V. Luchinsky, *Light hadron production in $B_c \to J/\psi + X$ decays*, *Phys. Rev. D* **81** (2010) 014015 [arXiv:0910.3089] [INSPIRE].

[27] A.V. Luchinsky, *Production of K mesons in exclusive B_c decays*, arXiv:1307.0953 [INSPIRE].

[28] A.K. Likhoded and A.V. Luchinsky, *Production of a pion system in exclusive $B_c \to V(P) + n\pi$ decays*, *Phys. Atom. Nucl.* **76** (2013) 787 [INSPIRE].

[29] LHCb collaboration, *The LHCb detector at the LHC*, 2008 *JINST* **3** S08005 [INSPIRE].

[30] LHCb collaboration, *LHCb detector performance*, *Int. J. Mod. Phys. A* **30** (2015) 1530022 [arXiv:1412.6352] [INSPIRE].

[31] R. Aaij et al., *Performance of the LHCb vertex locator*, 2014 *JINST* **9** P09007 [arXiv:1405.7808] [INSPIRE].

[32] R. Arink et al., *Performance of the LHCb Outer Tracker*, 2014 *JINST* **9** P01002 [arXiv:1311.3893] [INSPIRE].

[33] P. d'Argent et al., *Improved performance of the LHCb Outer Tracker in LHC Run 2*, 2017 *JINST* **12** P11016 [arXiv:1708.00819] [INSPIRE].

[34] LHCb collaboration, *Measurement of the Λ_b^0, Ξ_b^- and Ω_b^- baryon masses*, *Phys. Rev. Lett.* **110** (2013) 182001 [arXiv:1302.1072] [INSPIRE].

[35] LHCb collaboration, *Precision measurement of D meson mass differences*, *JHEP* **06** (2013) 065 [arXiv:1304.6865] [INSPIRE].

[36] M. Adinolfi et al., *Performance of the LHCb RICH detector at the LHC*, *Eur. Phys. J. C* **73** (2013) 2431 [arXiv:1211.6759] [INSPIRE].

[37] A.A. Alves Jr. et al., *Performance of the LHCb muon system*, 2013 *JINST* **8** P02022 [arXiv:1211.1346] [INSPIRE].

[38] R. Aaij et al., *The LHCb trigger and its performance in 2011*, 2013 *JINST* **8** P04022 [arXiv:1211.3055] [INSPIRE].

[39] T. Sjöstrand, S. Mrenna and P.Z. Skands, *A brief introduction to PYTHIA 8.1*, *Comput. Phys. Commun.* **178** (2008) 852 [`arXiv:0710.3820`] [ɪɴSPIRE].

[40] I. Belyaev et al., *Handling of the generation of primary events in Gauss, the LHCb simulation framework*, *J. Phys. Conf. Ser.* **331** (2011) 032047 [ɪɴSPIRE].

[41] D.J. Lange, *The EvtGen particle decay simulation package*, *Nucl. Instrum. Meth. A* **462** (2001) 152 [ɪɴSPIRE].

[42] N. Davidson, T. Przedzinski and Z. Was, *PHOTOS interface in C++: technical and physics documentation*, *Comput. Phys. Commun.* **199** (2016) 86 [`arXiv:1011.0937`] [ɪɴSPIRE].

[43] A.V. Berezhnoy, A.K. Likhoded and A.V. Luchinsky, *BC_NPI module for the analysis of $B_c \to J/\psi + n\pi$ and $B_c \to B_s + n\pi$ decays within the EvtGen package*, `arXiv:1104.0808` [ɪɴSPIRE].

[44] LHCb collaboration, *Observation of $J/\psi\phi$ structures consistent with exotic states from amplitude analysis of $B^+ \to J/\psi\phi K^+$ decays*, *Phys. Rev. Lett.* **118** (2017) 022003 [`arXiv:1606.07895`] [ɪɴSPIRE].

[45] LHCb collaboration, *Amplitude analysis of $B^+ \to J/\psi\phi K^+$ decays*, *Phys. Rev. D* **95** (2017) 012002 [`arXiv:1606.07898`] [ɪɴSPIRE].

[46] GEANT4 collaboration, *GEANT4 developments and applications*, *IEEE Trans. Nucl. Sci.* **53** (2006) 270 [ɪɴSPIRE].

[47] GEANT4 collaboration, *GEANT4 — a simulation toolkit*, *Nucl. Instrum. Meth. A* **506** (2003) 250 [ɪɴSPIRE].

[48] M. Clemencic et al., *The LHCb simulation application, Gauss: design, evolution and experience*, *J. Phys. Conf. Ser.* **331** (2011) 032023 [ɪɴSPIRE].

[49] LHCb collaboration, *Measurement of the track reconstruction efficiency at LHCb*, 2015 *JINST* **10** P02007 [`arXiv:1408.1251`] [ɪɴSPIRE].

[50] A. Powell, *Particle identification at LHCb*, `PoS(ICHEP2010)020` [ɪɴSPIRE].

[51] W.D. Hulsbergen, *Decay chain fitting with a Kalman filter*, *Nucl. Instrum. Meth. A* **552** (2005) 566 [`physics/0503191`] [ɪɴSPIRE].

[52] PARTICLE DATA GROUP collaboration, *Review of particle physics*, *PTEP* **2020** (2020) 083C01 [ɪɴSPIRE].

[53] LHCb collaboration, *Study of the $\psi_2(3823)$ and $\chi_{c1}(3872)$ states in $B^+ \to (J\psi\pi^+\pi^-) K^+$ decays*, *JHEP* **08** (2020) 123 [`arXiv:2005.13422`] [ɪɴSPIRE].

[54] LHCb collaboration, *Study of $B_s^0 \to J\psi\pi^+\pi^- K^+K^-$ decays*, *JHEP* **02** (2021) 024 [*Erratum ibid.* **04** (2021) 170] [`arXiv:2011.01867`] [ɪɴSPIRE].

[55] LHCb collaboration, *Observation of J/ψ pair production in pp collisions at $\sqrt{s} = 7$ TeV*, *Phys. Lett. B* **707** (2012) 52 [`arXiv:1109.0963`] [ɪɴSPIRE].

[56] T. Skwarnicki, *A study of the radiative cascade transitions between the Υ' and Υ resonances*, Ph.D. thesis, Institute of Nuclear Physics, Krakow, Poland (1986) [DESY-F31-86-02].

[57] E. Byckling and K. Kajantie, *Particle kinematics*, John Wiley & Sons Inc., New York, U.S.A (1973).

[58] LHCb collaboration, *Study of the lineshape of the $\chi_{c1}(3872)$ state*, *Phys. Rev. D* **102** (2020) 092005 [`arXiv:2005.13419`] [ɪɴSPIRE].

[59] M. Pivk and F.R. Le Diberder, *SPlot: a statistical tool to unfold data distributions*, *Nucl. Instrum. Meth. A* **555** (2005) 356 [physics/0402083] [INSPIRE].

[60] S.S. Wilks, *The large-sample distribution of the likelihood ratio for testing composite hypotheses*, *Annals Math. Statist.* **9** (1938) 60 [INSPIRE].

[61] CLEO collaboration, *Hadronic structure in the decay $\tau^- \to \nu_\tau \pi^- \pi^0 \pi^0$ and the sign of the tau-neutrino helicity*, *Phys. Rev. D* **61** (2000) 012002 [hep-ex/9902022] [INSPIRE].

[62] J.M. Blatt and V.F. Weisskopf, *Theoretical nuclear physics*, Springer, New York, Germany (1952) [INSPIRE].

[63] S. Okubo, *ϕ-meson and unitary symmetry model*, *Phys. Lett.* **5** (1963) 165 [INSPIRE].

[64] G. Zweig, *An SU_3 model for strong interaction symmetry and its breaking; Version 2*, CERN-TH-412 (1964).

[65] J. Iizuka, *A systematics and phenomenology of meson family*, *Prog. Theor. Phys. Suppl.* **37** (1966) 21 [INSPIRE].

[66] R. Aaij et al., *Selection and processing of calibration samples to measure the particle identification performance of the LHCb experiment in Run 2*, *EPJ Tech. Instrum.* **6** (2019) 1 [arXiv:1803.00824] [INSPIRE].

[67] D. Martínez Santos and F. Dupertuis, *Mass distributions marginalized over per-event errors*, *Nucl. Instrum. Meth. A* **764** (2014) 150 [arXiv:1312.5000] [INSPIRE].

[68] LHCb collaboration, *Measurement of relative branching fractions of B decays to $\psi(2S)$ and J/ψ mesons*, *Eur. Phys. J. C* **72** (2012) 2118 [arXiv:1205.0918] [INSPIRE].

[69] G.J. Gounaris and J.J. Sakurai, *Finite width corrections to the vector meson dominance prediction for $\rho \to e^+ e^-$*, *Phys. Rev. Lett.* **21** (1968) 244 [INSPIRE].

[70] LHCb collaboration, *First observation of the decays $\bar{B}^0 \to D^+ K^- \pi^+ \pi^-$ and $B^- \to D^0 K^- \pi^+ \pi^-$*, *Phys. Rev. Lett.* **108** (2012) 161801 [arXiv:1201.4402] [INSPIRE].

[71] LHCb collaboration, *Study of $B^0 \to D^{*-} \pi^+ \pi^- \pi^+$ and $B^0 \to D^{*-} K^+ \pi^- \pi^+$ decays*, *Phys. Rev. D* **87** (2013) 092001 [arXiv:1303.6861] [INSPIRE].

[72] LHCb collaboration, *First observation of the decays $\bar{B}^0_{(s)} \to D_s^+ K^- \pi^+ \pi^-$ and $\bar{B}^0_s \to D_{s1}(2536)^+ \pi^-$*, *Phys. Rev. D* **86** (2012) 112005 [arXiv:1211.1541] [INSPIRE].

The LHCb collaboration

R. Aaij[32], A.S.W. Abdelmotteleb[56], C. Abellán Beteta[50], F.J. Abudinen Gallego[56],
T. Ackernley[60], B. Adeva[46], M. Adinolfi[54], H. Afsharnia[9], C. Agapopoulou[13], C.A. Aidala[87],
S. Aiola[25], Z. Ajaltouni[9], S. Akar[65], J. Albrecht[15], F. Alessio[48], M. Alexander[59],
A. Alfonso Albero[45], Z. Aliouche[62], G. Alkhazov[38], P. Alvarez Cartelle[55], S. Amato[2],
J.L. Amey[54], Y. Amhis[11], L. An[48], L. Anderlini[22], A. Andreianov[38], M. Andreotti[21], F. Archilli[17],
A. Artamonov[44], M. Artuso[68], K. Arzymatov[42], E. Aslanides[10], M. Atzeni[50], B. Audurier[12],
S. Bachmann[17], M. Bachmayer[49], J.J. Back[56], P. Baladron Rodriguez[46], V. Balagura[12],
W. Baldini[21], J. Baptista Leite[1], M. Barbetti[22,h], R.J. Barlow[62], S. Barsuk[11], W. Barter[61],
M. Bartolini[24,i], F. Baryshnikov[83], J.M. Basels[14], S. Bashir[34], G. Bassi[29], B. Batsukh[68],
A. Battig[15], A. Bay[49], A. Beck[56], M. Becker[15], F. Bedeschi[29], I. Bediaga[1], A. Beiter[68],
V. Belavin[42], S. Belin[27], V. Bellee[50], K. Belous[44], I. Belov[40], I. Belyaev[41], G. Bencivenni[23],
E. Ben-Haim[13], A. Berezhnoy[40], R. Bernet[50], D. Berninghoff[17], H.C. Bernstein[68], C. Bertella[48],
A. Bertolin[28], C. Betancourt[50], F. Betti[48], Ia. Bezshyiko[50], S. Bhasin[54], J. Bhom[35], L. Bian[73],
M.S. Bieker[15], S. Bifani[53], P. Billoir[13], A. Biolchini[32], M. Birch[61], F.C.R. Bishop[55], A. Bitadze[62],
A. Bizzeti[22,l], M. Bjørn[63], M.P. Blago[48], T. Blake[56], F. Blanc[49], S. Blusk[68], D. Bobulska[59],
J.A. Boelhauve[15], O. Boente Garcia[46], T. Boettcher[65], A. Boldyrev[82], A. Bondar[43],
N. Bondar[38,48], S. Borghi[62], M. Borisyak[42], M. Borsato[17], J.T. Borsuk[35], S.A. Bouchiba[49],
T.J.V. Bowcock[60], A. Boyer[48], C. Bozzi[21], M.J. Bradley[61], S. Braun[66], A. Brea Rodriguez[46],
J. Brodzicka[35], A. Brossa Gonzalo[56], D. Brundu[27], A. Buonaura[50], L. Buonincontri[28],
A.T. Burke[62], C. Burr[48], A. Bursche[72], A. Butkevich[39], J.S. Butter[32], J. Buytaert[48],
W. Byczynski[48], S. Cadeddu[27], H. Cai[73], R. Calabrese[21,g], L. Calefice[15,13], S. Cali[23],
R. Calladine[53], M. Calvi[26,k], M. Calvo Gomez[85], P. Camargo Magalhaes[54], P. Campana[23],
A.F. Campoverde Quezada[6], S. Capelli[26,k], L. Capriotti[20,e], A. Carbone[20,e], G. Carboni[31,q],
R. Cardinale[24,i], A. Cardini[27], I. Carli[4], P. Carniti[26,k], L. Carus[14], K. Carvalho Akiba[32],
A. Casais Vidal[46], R. Caspary[17], G. Casse[60], M. Cattaneo[48], G. Cavallero[48], S. Celani[49],
J. Cerasoli[10], D. Cervenkov[63], A.J. Chadwick[60], M.G. Chapman[54], M. Charles[13],
Ph. Charpentier[48], G. Chatzikonstantinidis[53], C.A. Chavez Barajas[60], M. Chefdeville[8], C. Chen[3],
S. Chen[4], A. Chernov[35], V. Chobanova[46], S. Cholak[49], M. Chrzaszcz[35], A. Chubykin[38],
V. Chulikov[38], P. Ciambrone[23], M.F. Cicala[56], X. Cid Vidal[46], G. Ciezarek[48], P.E.L. Clarke[58],
M. Clemencic[48], H.V. Cliff[55], J. Closier[48], J.L. Cobbledick[62], V. Coco[48], J.A.B. Coelho[11],
J. Cogan[10], E. Cogneras[9], L. Cojocariu[37], P. Collins[48], T. Colombo[48], L. Congedo[19,d],
A. Contu[27], N. Cooke[53], G. Coombs[59], I. Corredoira [46], G. Corti[48], C.M. Costa Sobral[56],
B. Couturier[48], D.C. Craik[64], J. Crkovská[67], M. Cruz Torres[1], R. Currie[58], C.L. Da Silva[67],
S. Dadabaev[83], L. Dai[71], E. Dall'Occo[15], J. Dalseno[46], C. D'Ambrosio[48], A. Danilina[41],
P. d'Argent[48], A. Dashkina[83], J.E. Davies[62], A. Davis[62], O. De Aguiar Francisco[62],
K. De Bruyn[79], S. De Capua[62], M. De Cian[49], E. De Lucia[23], J.M. De Miranda[1], L. De Paula[2],
M. De Serio[19,d], D. De Simone[50], P. De Simone[23], F. De Vellis[15], J.A. de Vries[80], C.T. Dean[67],
F. Debernardis[19,d], D. Decamp[8], V. Dedu[10], L. Del Buono[13], B. Delaney[55], H.-P. Dembinski[15],
A. Dendek[34], V. Denysenko[50], D. Derkach[82], O. Deschamps[9], F. Desse[11], F. Dettori[27,f],
B. Dey[77], A. Di Cicco[23], P. Di Nezza[23], S. Didenko[83], L. Dieste Maronas[46], H. Dijkstra[48],
V. Dobishuk[52], C. Dong[3], A.M. Donohoe[18], F. Dordei[27], A.C. dos Reis[1], L. Douglas[59],
A. Dovbnya[51], A.G. Downes[8], M.W. Dudek[35], L. Dufour[48], V. Duk[78], P. Durante[48],
J.M. Durham[67], D. Dutta[62], A. Dziurda[35], A. Dzyuba[38], S. Easo[57], U. Egede[69], A. Egorychev[41],
V. Egorychev[41], S. Eidelman[43,v,†], S. Eisenhardt[58], S. Ek-In[49], L. Eklund[86], S. Ely[68], A. Ene[37],
E. Epple[67], S. Escher[14], J. Eschle[50], S. Esen[13], T. Evans[48], Y. Fan[6], B. Fang[73], S. Farry[60],
D. Fazzini[26,k], M. Féo[48], A. Fernandez Prieto[46], A.D. Fernez[66], F. Ferrari[20,e], L. Ferreira Lopes[49],

F. Ferreira Rodrigues[2], S. Ferreres Sole[32], M. Ferrillo[50], M. Ferro-Luzzi[48], S. Filippov[39],
R.A. Fini[19], M. Fiorini[21,g], M. Firlej[34], K.M. Fischer[63], D.S. Fitzgerald[87], C. Fitzpatrick[62],
T. Fiutowski[34], A. Fkiaras[48], F. Fleuret[12], M. Fontana[13], F. Fontanelli[24,i], R. Forty[48],
D. Foulds-Holt[55], V. Franco Lima[60], M. Franco Sevilla[66], M. Frank[48], E. Franzoso[21], G. Frau[17],
C. Frei[48], D.A. Friday[59], J. Fu[6], Q. Fuehring[15], E. Gabriel[32], G. Galati[19,d], A. Gallas Torreira[46],
D. Galli[20,e], S. Gambetta[58,48], Y. Gan[3], M. Gandelman[2], P. Gandini[25], Y. Gao[5], M. Garau[27],
L.M. Garcia Martin[56], P. Garcia Moreno[45], J. García Pardiñas[26,k], B. Garcia Plana[46],
F.A. Garcia Rosales[12], L. Garrido[45], C. Gaspar[48], R.E. Geertsema[32], D. Gerick[17], L.L. Gerken[15],
E. Gersabeck[62], M. Gersabeck[62], T. Gershon[56], D. Gerstel[10], L. Giambastiani[28], V. Gibson[55],
H.K. Giemza[36], A.L. Gilman[63], M. Giovannetti[23,q], A. Gioventù[46], P. Gironella Gironell[45],
C. Giugliano[21,g,48], K. Gizdov[58], E.L. Gkougkousis[48], V.V. Gligorov[13], C. Göbel[70],
E. Golobardes[85], D. Golubkov[41], A. Golutvin[61,83], A. Gomes[1,a], S. Gomez Fernandez[45],
F. Goncalves Abrantes[63], M. Goncerz[35], G. Gong[3], P. Gorbounov[41], I.V. Gorelov[40], C. Gotti[26],
E. Govorkova[48], J.P. Grabowski[17], T. Grammatico[13], L.A. Granado Cardoso[48], E. Graugés[45],
E. Graverini[49], G. Graziani[22], A. Grecu[37], L.M. Greeven[32], N.A. Grieser[4], L. Grillo[62],
S. Gromov[83], B.R. Gruberg Cazon[63], C. Gu[3], M. Guarise[21], M. Guittiere[11], P.A. Günther[17],
E. Gushchin[39], A. Guth[14], Y. Guz[44], T. Gys[48], T. Hadavizadeh[69], G. Haefeli[49], C. Haen[48],
J. Haimberger[48], T. Halewood-leagas[60], P.M. Hamilton[66], J.P. Hammerich[60], Q. Han[7], X. Han[17],
T.H. Hancock[63], E.B. Hansen[62], S. Hansmann-Menzemer[17], N. Harnew[63], T. Harrison[60],
C. Hasse[48], M. Hatch[48], J. He[6,b], M. Hecker[61], K. Heijhoff[32], K. Heinicke[15], R.D.L. Henderson[69],
A.M. Hennequin[48], K. Hennessy[60], L. Henry[48], J. Heuel[14], A. Hicheur[2], D. Hill[49], M. Hilton[62],
S.E. Hollitt[15], R. Hou[7], Y. Hou[8], J. Hu[17], J. Hu[72], W. Hu[7], X. Hu[3], W. Huang[6], X. Huang[73],
W. Hulsbergen[32], R.J. Hunter[56], M. Hushchyn[82], D. Hutchcroft[60], D. Hynds[32], P. Ibis[15],
M. Idzik[34], D. Ilin[38], P. Ilten[65], A. Inglessi[38], A. Ishteev[83], K. Ivshin[38], R. Jacobsson[48], H. Jage[14],
S. Jakobsen[48], E. Jans[32], B.K. Jashal[47], A. Jawahery[66], V. Jevtic[15], X. Jiang[4], M. John[63],
D. Johnson[64], C.R. Jones[55], T.P. Jones[56], B. Jost[48], N. Jurik[48], S.H. Kalavan Kadavath[34],
S. Kandybei[51], Y. Kang[3], M. Karacson[48], M. Karpov[82], F. Keizer[48], D.M. Keller[68], M. Kenzie[56],
T. Ketel[33], B. Khanji[15], A. Kharisova[84], S. Kholodenko[44], T. Kirn[14], V.S. Kirsebom[49],
O. Kitouni[64], S. Klaver[32], N. Kleijne[29], K. Klimaszewski[36], M.R. Kmiec[36], S. Koliiev[52],
A. Kondybayeva[83], A. Konoplyannikov[41], P. Kopciewicz[34], R. Kopecna[17], P. Koppenburg[32],
M. Korolev[40], I. Kostiuk[32,52], O. Kot[52], S. Kotriakhova[21,38], P. Kravchenko[38], L. Kravchuk[39],
R.D. Krawczyk[48], M. Kreps[56], F. Kress[61], S. Kretzschmar[14], P. Krokovny[43,v], W. Krupa[34],
W. Krzemien[36], J. Kubat[17], M. Kucharczyk[35], V. Kudryavtsev[43,v], H.S. Kuindersma[32,33],
G.J. Kunde[67], T. Kvaratskheliya[41], D. Lacarrere[48], G. Lafferty[62], A. Lai[27], A. Lampis[27],
D. Lancierini[50], J.J. Lane[62], R. Lane[54], G. Lanfranchi[23], C. Langenbruch[14], J. Langer[15],
O. Lantwin[83], T. Latham[56], F. Lazzari[29,r], R. Le Gac[10], S.H. Lee[87], R. Lefèvre[9], A. Leflat[40],
S. Legotin[83], O. Leroy[10], T. Lesiak[35], B. Leverington[17], H. Li[72], P. Li[17], S. Li[7], Y. Li[4], Y. Li[4],
Z. Li[68], X. Liang[68], T. Lin[61], R. Lindner[48], V. Lisovskyi[15], R. Litvinov[27], G. Liu[72], H. Liu[6],
Q. Liu[6], S. Liu[4], A. Lobo Salvia[45], A. Loi[27], J. Lomba Castro[46], I. Longstaff[59], J.H. Lopes[2],
S. Lopez Solino[46], G.H. Lovell[55], Y. Lu[4], C. Lucarelli[22,h], D. Lucchesi[28,m], S. Luchuk[39],
M. Lucio Martinez[32], V. Lukashenko[32,52], Y. Luo[3], A. Lupato[62], E. Luppi[21,g], O. Lupton[56],
A. Lusiani[29,n], X. Lyu[6], L. Ma[4], R. Ma[6], S. Maccolini[20,e], F. Machefert[11], F. Maciuc[37],
V. Macko[49], P. Mackowiak[15], S. Maddrell-Mander[54], O. Madejczyk[34], L.R. Madhan Mohan[54],
O. Maev[38], A. Maevskiy[82], D. Maisuzenko[38], M.W. Majewski[34], J.J. Malczewski[35], S. Malde[63],
B. Malecki[48], A. Malinin[81], T. Maltsev[43,v], H. Malygina[17], G. Manca[27,f], G. Mancinelli[10],
D. Manuzzi[20,e], D. Marangotto[25,j], J. Maratas[9,t], J.F. Marchand[8], U. Marconi[20], S. Mariani[22,h],
C. Marin Benito[48], M. Marinangeli[49], J. Marks[17], A.M. Marshall[54], P.J. Marshall[60],
G. Martelli[78], G. Martellotti[30], L. Martinazzoli[48,k], M. Martinelli[26,k], D. Martinez Santos[46],

F. Martinez Vidal[47], A. Massafferri[1], M. Materok[14], R. Matev[48], A. Mathad[50], V. Matiunin[41],
C. Matteuzzi[26], K.R. Mattioli[87], A. Mauri[32], E. Maurice[12], J. Mauricio[45], M. Mazurek[48],
M. McCann[61], L. Mcconnell[18], T.H. Mcgrath[62], N.T. Mchugh[59], A. McNab[62], R. McNulty[18],
J.V. Mead[60], B. Meadows[65], G. Meier[15], N. Meinert[76], D. Melnychuk[36], S. Meloni[26,k],
M. Merk[32,80], A. Merli[25,j], L. Meyer Garcia[2], M. Mikhasenko[75,c], D.A. Milanes[74], E. Millard[56],
M. Milovanovic[48], M.-N. Minard[8], A. Minotti[26,k], L. Minzoni[21,g], S.E. Mitchell[58], B. Mitreska[62],
D.S. Mitzel[15], A. Mödden [15], R.A. Mohammed[63], R.D. Moise[61], S. Mokhnenko[82],
T. Mombächer[46], I.A. Monroy[74], S. Monteil[9], M. Morandin[28], G. Morello[23], M.J. Morello[29,n],
J. Moron[34], A.B. Morris[75], A.G. Morris[56], R. Mountain[68], H. Mu[3], F. Muheim[58,48], M. Mulder[48],
D. Müller[48], K. Müller[50], C.H. Murphy[63], D. Murray[62], R. Murta[61], P. Muzzetto[27,48], P. Naik[54],
T. Nakada[49], R. Nandakumar[57], T. Nanut[49], I. Nasteva[2], M. Needham[58], N. Neri[25,j],
S. Neubert[75], N. Neufeld[48], R. Newcombe[61], E.M. Niel[11], S. Nieswand[14], N. Nikitin[40],
N.S. Nolte[64], C. Normand[8], C. Nunez[87], A. Oblakowska-Mucha[34], V. Obraztsov[44], T. Oeser[14],
D.P. O'Hanlon[54], S. Okamura[21], R. Oldeman[27,f], F. Oliva[58], M.E. Olivares[68],
C.J.G. Onderwater[79], R.H. O'Neil[58], J.M. Otalora Goicochea[2], T. Ovsiannikova[41], P. Owen[50],
A. Oyanguren[47], K.O. Padeken[75], B. Pagare[56], P.R. Pais[48], T. Pajero[63], A. Palano[19],
M. Palutan[23], Y. Pan[62], G. Panshin[84], A. Papanestis[57], M. Pappagallo[19,d], L.L. Pappalardo[21,g],
C. Pappenheimer[65], W. Parker[66], C. Parkes[62], B. Passalacqua[21], G. Passaleva[22], A. Pastore[19],
M. Patel[61], C. Patrignani[20,e], C.J. Pawley[80], A. Pearce[48,57], A. Pellegrino[32], M. Pepe Altarelli[48],
S. Perazzini[20], D. Pereima[41], A. Pereiro Castro[46], P. Perret[9], M. Petric[59,48], K. Petridis[54],
A. Petrolini[24,i], A. Petrov[81], S. Petrucci[58], M. Petruzzo[25], T.T.H. Pham[68], A. Philippov[42],
L. Pica[29,n], M. Piccini[78], B. Pietrzyk[8], G. Pietrzyk[49], M. Pili[63], D. Pinci[30], F. Pisani[48],
M. Pizzichemi[26,48,k], P.K. Resmi[10], V. Placinta[37], J. Plews[53], M. Plo Casasus[46], F. Polci[13],
M. Poli Lener[23], M. Poliakova[68], A. Poluektov[10], N. Polukhina[83,u], I. Polyakov[68], E. Polycarpo[2],
S. Ponce[48], D. Popov[6,48], S. Popov[42], S. Poslavskii[44], K. Prasanth[35], L. Promberger[48],
C. Prouve[46], V. Pugatch[52], V. Puill[11], H. Pullen[63], G. Punzi[29,o], H. Qi[3], W. Qian[6], J. Qin[6],
N. Qin[3], R. Quagliani[49], B. Quintana[8], N.V. Raab[18], R.I. Rabadan Trejo[6], B. Rachwal[34],
J.H. Rademacker[54], M. Rama[29], M. Ramos Pernas[56], M.S. Rangel[2], F. Ratnikov[42,82], G. Raven[33],
M. Reboud[8], F. Redi[49], F. Reiss[62], C. Remon Alepuz[47], Z. Ren[3], V. Renaudin[63], R. Ribatti[29],
S. Ricciardi[57], K. Rinnert[60], P. Robbe[11], G. Robertson[58], A.B. Rodrigues[49], E. Rodrigues[60],
J.A. Rodriguez Lopez[74], E.R.R. Rodriguez Rodriguez[46], A. Rollings[63], P. Roloff[48],
V. Romanovskiy[44], M. Romero Lamas[46], A. Romero Vidal[46], J.D. Roth[87], M. Rotondo[23],
M.S. Rudolph[68], T. Ruf[48], R.A. Ruiz Fernandez[46], J. Ruiz Vidal[47], A. Ryzhikov[82], J. Ryzka[34],
J.J. Saborido Silva[46], N. Sagidova[38], N. Sahoo[56], B. Saitta[27,f], M. Salomoni[48], C. Sanchez Gras[32],
R. Santacesaria[30], C. Santamarina Rios[46], M. Santimaria[23], E. Santovetti[31,q], D. Saranin[83],
G. Sarpis[14], M. Sarpis[75], A. Sarti[30], C. Satriano[30,p], A. Satta[31], M. Saur[15], D. Savrina[41,40],
H. Sazak[9], L.G. Scantlebury Smead[63], A. Scarabotto[13], S. Schael[14], S. Scherl[60], M. Schiller[59],
H. Schindler[48], M. Schmelling[16], B. Schmidt[48], S. Schmitt[14], O. Schneider[49], A. Schopper[48],
M. Schubiger[32], S. Schulte[49], M.H. Schune[11], R. Schwemmer[48], B. Sciascia[23,48], S. Sellam[46],
A. Semennikov[41], M. Senghi Soares[33], A. Sergi[24,i], N. Serra[50], L. Sestini[28], A. Seuthe[15],
Y. Shang[5], D.M. Shangase[87], M. Shapkin[44], I. Shchemerov[83], L. Shchutska[49], T. Shears[60],
L. Shekhtman[43,v], Z. Shen[5], S. Sheng[4], V. Shevchenko[81], E.B. Shields[26,k], Y. Shimizu[11],
E. Shmanin[83], J.D. Shupperd[68], B.G. Siddi[21], R. Silva Coutinho[50], G. Simi[28], S. Simone[19,d],
N. Skidmore[62], T. Skwarnicki[68], M.W. Slater[53], I. Slazyk[21,g], J.C. Smallwood[63], J.G. Smeaton[55],
A. Smetkina[41], E. Smith[50], M. Smith[61], A. Snoch[32], L. Soares Lavra[9], M.D. Sokoloff[65],
F.J.P. Soler[59], A. Solovev[38], I. Solovyev[38], F.L. Souza De Almeida[2], B. Souza De Paula[2],
B. Spaan[15], E. Spadaro Norella[25,j], P. Spradlin[59], F. Stagni[48], M. Stahl[65], S. Stahl[48],
S. Stanislaus[63], O. Steinkamp[50,83], O. Stenyakin[44], H. Stevens[15], S. Stone[68], D. Strekalina[83],

F. Suljik[63], J. Sun[27], L. Sun[73], Y. Sun[66], P. Svihra[62], P.N. Swallow[53], K. Swientek[34],
A. Szabelski[36], T. Szumlak[34], M. Szymanski[48], S. Taneja[62], A.R. Tanner[54], M.D. Tat[63],
A. Terentev[83], F. Teubert[48], E. Thomas[48], D.J.D. Thompson[53], K.A. Thomson[60], H. Tilquin[61],
V. Tisserand[9], S. T'Jampens[8], M. Tobin[4], L. Tomassetti[21,g], X. Tong[5], D. Torres Machado[1],
D.Y. Tou[13], E. Trifonova[83], C. Trippl[49], G. Tuci[6], A. Tully[49], N. Tuning[32,48], A. Ukleja[36],
D.J. Unverzagt[17], E. Ursov[83], A. Usachov[32], A. Ustyuzhanin[42,82], U. Uwer[17], A. Vagner[84],
V. Vagnoni[20], A. Valassi[48], G. Valenti[20], N. Valls Canudas[85], M. van Beuzekom[32], M. Van Dijk[49],
H. Van Hecke[67], E. van Herwijnen[83], M. van Veghel[79], R. Vazquez Gomez[45],
P. Vazquez Regueiro[46], C. Vázquez Sierra[48], S. Vecchi[21], J.J. Velthuis[54], M. Veltri[22,s],
A. Venkateswaran[68], M. Veronesi[32], M. Vesterinen[56], D. Vieira[65], M. Vieites Diaz[49],
H. Viemann[76], X. Vilasis-Cardona[85], E. Vilella Figueras[60], A. Villa[20], P. Vincent[13], F.C. Volle[11],
D. Vom Bruch[10], A. Vorobyev[38], V. Vorobyev[43,v], N. Voropaev[38], K. Vos[80], R. Waldi[17],
J. Walsh[29], C. Wang[17], J. Wang[5], J. Wang[4], J. Wang[3], J. Wang[73], M. Wang[3], R. Wang[54],
Y. Wang[7], Z. Wang[50], Z. Wang[3], Z. Wang[6], J.A. Ward[56], N.K. Watson[53], S.G. Weber[13],
D. Websdale[61], C. Weisser[64], B.D.C. Westhenry[54], D.J. White[62], M. Whitehead[54],
A.R. Wiederhold[56], D. Wiedner[15], G. Wilkinson[63], M. Wilkinson[68], I. Williams[55], M. Williams[64],
M.R.J. Williams[58], F.F. Wilson[57], W. Wislicki[36], M. Witek[35], L. Witola[17], G. Wormser[11],
S.A. Wotton[55], H. Wu[68], K. Wyllie[48], Z. Xiang[6], D. Xiao[7], Y. Xie[7], A. Xu[5], J. Xu[6], L. Xu[3],
M. Xu[7], Q. Xu[6], Z. Xu[5], Z. Xu[6], D. Yang[3], S. Yang[6], Y. Yang[6], Z. Yang[5], Z. Yang[66], Y. Yao[68],
L.E. Yeomans[60], H. Yin[7], J. Yu[71], X. Yuan[68], O. Yushchenko[44], E. Zaffaroni[49], M. Zavertyaev[16,u],
M. Zdybal[35], O. Zenaiev[48], M. Zeng[3], D. Zhang[7], L. Zhang[3], S. Zhang[71], S. Zhang[5], Y. Zhang[5],
Y. Zhang[63], A. Zharkova[83], A. Zhelezov[17], Y. Zheng[6], T. Zhou[5], X. Zhou[6], Y. Zhou[6],
V. Zhovkovska[11], X. Zhu[3], X. Zhu[7], Z. Zhu[6], V. Zhukov[14,40], J.B. Zonneveld[58], Q. Zou[4],
S. Zucchelli[20,e], D. Zuliani[28], G. Zunica[62]

1   Centro Brasileiro de Pesquisas Físicas (CBPF), Rio de Janeiro, Brazil
2   Universidade Federal do Rio de Janeiro (UFRJ), Rio de Janeiro, Brazil
3   Center for High Energy Physics, Tsinghua University, Beijing, China
4   Institute Of High Energy Physics (IHEP), Beijing, China
5   School of Physics State Key Laboratory of Nuclear Physics and Technology, Peking University,
    Beijing, China
6   University of Chinese Academy of Sciences, Beijing, China
7   Institute of Particle Physics, Central China Normal University, Wuhan, Hubei, China
8   Univ. Savoie Mont Blanc, CNRS, IN2P3-LAPP, Annecy, France
9   Université Clermont Auvergne, CNRS/IN2P3, LPC, Clermont-Ferrand, France
10 Aix Marseille Univ, CNRS/IN2P3, CPPM, Marseille, France
11 Université Paris-Saclay, CNRS/IN2P3, IJCLab, Orsay, France
12 Laboratoire Leprince-Ringuet, CNRS/IN2P3, Ecole Polytechnique, Institut Polytechnique de Paris,
    Palaiseau, France
13 LPNHE, Sorbonne Université, Paris Diderot Sorbonne Paris Cité, CNRS/IN2P3, Paris, France
14 I. Physikalisches Institut, RWTH Aachen University, Aachen, Germany
15 Fakultät Physik, Technische Universität Dortmund, Dortmund, Germany
16 Max-Planck-Institut für Kernphysik (MPIK), Heidelberg, Germany
17 Physikalisches Institut, Ruprecht-Karls-Universität Heidelberg, Heidelberg, Germany
18 School of Physics, University College Dublin, Dublin, Ireland
19 INFN Sezione di Bari, Bari, Italy
20 INFN Sezione di Bologna, Bologna, Italy
21 INFN Sezione di Ferrara, Ferrara, Italy
22 INFN Sezione di Firenze, Firenze, Italy
23 INFN Laboratori Nazionali di Frascati, Frascati, Italy
24 INFN Sezione di Genova, Genova, Italy

[25] INFN Sezione di Milano, Milano, Italy

[26] INFN Sezione di Milano-Bicocca, Milano, Italy

[27] INFN Sezione di Cagliari, Monserrato, Italy

[28] Universita degli Studi di Padova, Universita e INFN, Padova, Padova, Italy

[29] INFN Sezione di Pisa, Pisa, Italy

[30] INFN Sezione di Roma La Sapienza, Roma, Italy

[31] INFN Sezione di Roma Tor Vergata, Roma, Italy

[32] Nikhef National Institute for Subatomic Physics, Amsterdam, Netherlands

[33] Nikhef National Institute for Subatomic Physics and VU University Amsterdam, Amsterdam, Netherlands

[34] AGH — University of Science and Technology, Faculty of Physics and Applied Computer Science, Kraków, Poland

[35] Henryk Niewodniczanski Institute of Nuclear Physics Polish Academy of Sciences, Kraków, Poland

[36] National Center for Nuclear Research (NCBJ), Warsaw, Poland

[37] Horia Hulubei National Institute of Physics and Nuclear Engineering, Bucharest-Magurele, Romania

[38] Petersburg Nuclear Physics Institute NRC Kurchatov Institute (PNPI NRC KI), Gatchina, Russia

[39] Institute for Nuclear Research of the Russian Academy of Sciences (INR RAS), Moscow, Russia

[40] Institute of Nuclear Physics, Moscow State University (SINP MSU), Moscow, Russia

[41] Institute of Theoretical and Experimental Physics NRC Kurchatov Institute (ITEP NRC KI), Moscow, Russia

[42] Yandex School of Data Analysis, Moscow, Russia

[43] Budker Institute of Nuclear Physics (SB RAS), Novosibirsk, Russia

[44] Institute for High Energy Physics NRC Kurchatov Institute (IHEP NRC KI), Protvino, Russia, Protvino, Russia

[45] ICCUB, Universitat de Barcelona, Barcelona, Spain

[46] Instituto Galego de Física de Altas Enerxías (IGFAE), Universidade de Santiago de Compostela, Santiago de Compostela, Spain

[47] Instituto de Fisica Corpuscular, Centro Mixto Universidad de Valencia — CSIC, Valencia, Spain

[48] European Organization for Nuclear Research (CERN), Geneva, Switzerland

[49] Institute of Physics, Ecole Polytechnique Fédérale de Lausanne (EPFL), Lausanne, Switzerland

[50] Physik-Institut, Universität Zürich, Zürich, Switzerland

[51] NSC Kharkiv Institute of Physics and Technology (NSC KIPT), Kharkiv, Ukraine

[52] Institute for Nuclear Research of the National Academy of Sciences (KINR), Kyiv, Ukraine

[53] University of Birmingham, Birmingham, United Kingdom

[54] H.H. Wills Physics Laboratory, University of Bristol, Bristol, United Kingdom

[55] Cavendish Laboratory, University of Cambridge, Cambridge, United Kingdom

[56] Department of Physics, University of Warwick, Coventry, United Kingdom

[57] STFC Rutherford Appleton Laboratory, Didcot, United Kingdom

[58] School of Physics and Astronomy, University of Edinburgh, Edinburgh, United Kingdom

[59] School of Physics and Astronomy, University of Glasgow, Glasgow, United Kingdom

[60] Oliver Lodge Laboratory, University of Liverpool, Liverpool, United Kingdom

[61] Imperial College London, London, United Kingdom

[62] Department of Physics and Astronomy, University of Manchester, Manchester, United Kingdom

[63] Department of Physics, University of Oxford, Oxford, United Kingdom

[64] Massachusetts Institute of Technology, Cambridge, MA, United States

[65] University of Cincinnati, Cincinnati, OH, United States

[66] University of Maryland, College Park, MD, United States

[67] Los Alamos National Laboratory (LANL), Los Alamos, United States

[68] Syracuse University, Syracuse, NY, United States

[69] School of Physics and Astronomy, Monash University, Melbourne, Australia, associated to [56]

[70] Pontifícia Universidade Católica do Rio de Janeiro (PUC-Rio), Rio de Janeiro, Brazil, associated to [2]

71 *Physics and Micro Electronic College, Hunan University, Changsha City, China, associated to* [7]

72 *Guangdong Provincial Key Laboratory of Nuclear Science, Guangdong-Hong Kong Joint Laboratory of Quantum Matter, Institute of Quantum Matter, South China Normal University, Guangzhou, China, associated to* [3]

73 *School of Physics and Technology, Wuhan University, Wuhan, China, associated to* [3]

74 *Departamento de Fisica, Universidad Nacional de Colombia, Bogota, Colombia, associated to* [13]

75 *Universität Bonn — Helmholtz-Institut für Strahlen und Kernphysik, Bonn, Germany, associated to* [17]

76 *Institut für Physik, Universität Rostock, Rostock, Germany, associated to* [17]

77 *Eotvos Lorand University, Budapest, Hungary, associated to* [48]

78 *INFN Sezione di Perugia, Perugia, Italy, associated to* [21]

79 *Van Swinderen Institute, University of Groningen, Groningen, Netherlands, associated to* [32]

80 *Universiteit Maastricht, Maastricht, Netherlands, associated to* [32]

81 *National Research Centre Kurchatov Institute, Moscow, Russia, associated to* [41]

82 *National Research University Higher School of Economics, Moscow, Russia, associated to* [42]

83 *National University of Science and Technology "MISIS", Moscow, Russia, associated to* [41]

84 *National Research Tomsk Polytechnic University, Tomsk, Russia, associated to* [41]

85 *DS4DS, La Salle, Universitat Ramon Llull, Barcelona, Spain, associated to* [45]

86 *Department of Physics and Astronomy, Uppsala University, Uppsala, Sweden, associated to* [59]

87 *University of Michigan, Ann Arbor, United States, associated to* [68]

a *Universidade Federal do Triângulo Mineiro (UFTM), Uberaba-MG, Brazil*

b *Hangzhou Institute for Advanced Study, UCAS, Hangzhou, China*

c *Excellence Cluster ORIGINS, Munich, Germany*

d *Università di Bari, Bari, Italy*

e *Università di Bologna, Bologna, Italy*

f *Università di Cagliari, Cagliari, Italy*

g *Università di Ferrara, Ferrara, Italy*

h *Università di Firenze, Firenze, Italy*

i *Università di Genova, Genova, Italy*

j *Università degli Studi di Milano, Milano, Italy*

k *Università di Milano Bicocca, Milano, Italy*

l *Università di Modena e Reggio Emilia, Modena, Italy*

m *Università di Padova, Padova, Italy*

n *Scuola Normale Superiore, Pisa, Italy*

o *Università di Pisa, Pisa, Italy*

p *Università della Basilicata, Potenza, Italy*

q *Università di Roma Tor Vergata, Roma, Italy*

r *Università di Siena, Siena, Italy*

s *Università di Urbino, Urbino, Italy*

t *MSU — Iligan Institute of Technology (MSU-IIT), Iligan, Philippines*

u *P.N. Lebedev Physical Institute, Russian Academy of Science (LPI RAS), Moscow, Russia*

v *Novosibirsk State University, Novosibirsk, Russia*

† *Deceased*